

Limitations of a superchiral field

Joseph S. Choi¹ and Minhaeng Cho^{2,3,*}¹The Institute of Optics, University of Rochester, Rochester, New York 14627, USA²Department of Chemistry, Korea University, Seoul 136-713, Korea³Multidimensional Spectroscopy Laboratory, Korea Basic Science Institute, Seoul 136-713, Korea

(Received 19 September 2012; published 27 December 2012)

Recently, Tang and Cohen [Y. Tang and A. E. Cohen, *Science* **332**, 333 (2011)] proposed and demonstrated the use of “superchiral” electromagnetic fields to enhance optical enantioselectivity. Their work generated much excitement as enantioselective signals are typically quite small, and it appeared that the enhancement factor could be extremely large. In this paper we explicitly show the limitations of such fields by including the magnetic susceptibility term. This term is small and is ignored in most cases compared to the electric polarizability term. However, for the fields used, the enhancement was obtained at the electric field energy node. Due to conservation of field energy, the magnetic field energy is then maximum, and the magnetic susceptibility contribution can no longer be ignored. This then is what limits the enhancement of the optical enantioselectivity. For a counterpropagating left- and right-circularly polarized light field, as used in the aforementioned experiment, we show that this fundamentally limits the enhancement to one or two orders of magnitude in general, determined by the ratio of the magnetic susceptibility to the electric polarizability of the material used. We also generalize the dissymmetry factor to include optical rotation effects present in chiral media, as opposed to fields being in vacuum. In the process, we generalize Lipkin’s “ Z^{000} zilch” (or “optical chirality”) to that for a linear medium. This generalization shows that chirality of the material cannot be completely separated from chirality of the field and that opposite enantiomers are symmetric in terms of the dissymmetry factor enhancement. Finally, an analogy between ellipsometric chiroptical signal enhancement and enhanced optical enantioselectivity using a standing wave chiral field is discussed. Our analysis and generalization can be used as a guide for future searches of locally enhanced chiral fields.

DOI: [10.1103/PhysRevA.86.063834](https://doi.org/10.1103/PhysRevA.86.063834)

PACS number(s): 33.55.+b, 42.25.Ja, 78.20.Ek, 42.50.Ct

I. INTRODUCTION

Optical activity stems from chiral molecules interacting differently to left-circularly polarized light (LCPL) versus right-circularly polarized light (RCPL). Enantiomers, which are nonsuperimposable mirror images of each other, are usually distinguished by circular dichroism (CD) spectroscopy, which measures the differential absorption rates. Because of this link between handedness of the materials and handedness of the fields, optical activity spectroscopy is typically used to provide important stereoscopic structural information about chemical and biological systems. However, chiral enantiomers are difficult to distinguish due to their small differences in response to LCPL and RCPL (10^{-6} – 10^{-4} smaller than absorption).

A metric appropriate for measuring the enantioselectivity of a system is the dimensionless *dissymmetry factor*. This was proposed by Kuhn and is defined as

$$g = \frac{\epsilon^L - \epsilon^R}{\epsilon} = \frac{\epsilon^L - \epsilon^R}{\frac{1}{2}(\epsilon^L + \epsilon^R)}, \quad (1)$$

where the superscripts L and R are for LCPL and RCPL, respectively, and ϵ is the *decadic molar extinction coefficient*. The dissymmetry factor can be described as the ratio of CD to the conventional absorption. The dissymmetry factor g is then a proper criterion, given the available instrumental sensitivity, for determining whether the CD is measurable for a particular

absorption band [1]. Recently, another type of dissymmetry factor was considered to determine possible enhancements of chiral fields in Refs. [2] and [3]. Their definition is essentially the same,

$$g \equiv \frac{A^+ - A^-}{\frac{1}{2}(A^+ + A^-)}, \quad (2)$$

where A^\pm is the absorption rate of left (+)- or right (–)-handed fields.

Tang and Cohen, in Refs. [2] and [3], have recently proposed a creative method to enhance enantioselectivity using what they termed a “superchiral” optical field, where a standing wave was created by reflecting a circularly polarized light (CPL) to create two oppositely handed, counterpropagating CPLs. In this paper, we refer to this arrangement as a standing wave chiral field (SWCF). They began with what they termed the “optical chirality” C , as defined originally by Lipkin (Z^{000} “zilch”) [3,4]:

$$C \equiv \frac{\epsilon_0}{2} \mathbf{E} \cdot \nabla \times \mathbf{E} + \frac{1}{2\mu_0} \mathbf{B} \cdot \nabla \times \mathbf{B}. \quad (3)$$

This and other zilches are conserved quantities in vacuum, according to the Maxwell equations. However, Lipkin and his contemporaries dismissed this zilch and others as physically irrelevant (although they did note that their zilch set has opposite signs for opposite CPLs) [4–7]. Recently, others have investigated this optical chirality and its connection to the helicity and angular momentum of the field further [8,9]. In particular, Cameron, Barnett, and Yao have interpreted Lipkin’s zilches to represent the “angular momentum” of

*Corresponding author: mcho@korea.ac.kr

the curl of the electromagnetic field instead of the angular momentum of the field itself [10,11].

The dissymmetry factor defined in Eq. (2) is then shown to be [3]

$$g = g_{\text{CPL}} \left(\frac{cC}{2\omega U_e} \right), \quad (4)$$

where g_{CPL} is the dissymmetry factor for a CPL, c is the speed of light, C is the optical chirality, ω is the angular frequency, and U_e is the time-averaged electric energy density. In Eq. (4), the material properties (g_{CPL}) can be separated from the incident electromagnetic (EM) field properties (in parentheses). Thus, to enhance the enantioselective dissymmetry factor, the field chirality term, $(cC)/(2\omega U_e)$ can be increased by reducing the electric energy density. Reference [3] proposes to accomplish this by creating the SWCF. Then, by placing the chiral molecules at the node of the electric field energy density, because C/U_e is inversely proportional to the amplitude of the net electric field component at the node, the dissymmetry factor is increased compared to its CPL value. The idea was ingenious in its simplicity.

The dissymmetry factor g for the experiment in Ref. [2] was then proposed to be

$$\frac{g}{g_{\text{CPL}}} \simeq \frac{1 + \sqrt{R}}{1 - \sqrt{R}}, \quad (5)$$

where $R \equiv (E_2/E_1)^2$ is the *reflectivity* of a mirror used to generate the SWCF, with E_2 being the electric field amplitude of the reflected wave and E_1 being the amplitude of the incident electric field. Thus, according to this proposed formula, by selecting a highly reflective mirror, the enhancement factor can be quite large, if not infinite. The theory was further expanded to include the quadrupole contribution in oriented samples, which was shown to provide the same enhancement [12].

This theory was subsequently tested experimentally, by conducting the SWCF experiment proposed [2]. A mirror with reflectivity $R = 0.72$ was used and their results showed that $g_{\text{max}}/g_{\text{CPL}}$ was 10.6 ± 0.6 for the “p” enantiomer and 11.6 ± 0.6 for the “m” enantiomer. This was about 5%–13% different from the theoretical value of 12.2 from Eq. (5). Thus, an order of magnitude improvement in the dissymmetry factor was achieved when compared to a standard CD spectroscopic measurement.

After this theory for SWCF to increase enantioselectivity was published [3,13], Hendry *et al.* independently demonstrated a 10^6 enhancement in chiroptical refractive index differences between LCPL and RCPL, that is, *optical rotatory dispersion* (ORD), than that obtained by just using CPLs. This effect was demonstrated using two-dimensional nanocrosses with different “handedness” in the cross directions. They also called their fields “superchiral,” following the terminology from Ref. [3]. Using the same optical chirality C , they stated that C is increased by about two orders of magnitude than that from CPL’s at the near fields of the nanostructures used. They then suggested that the other four orders of magnitude might come from steep gradients of the structure, attributable to the electric-dipole electric-quadrupole contribution, though this is not a certainty. Following their experimental work, Hendry *et al.* presented a modal matching theory to describe their

nanodevices by analyzing when and how the chirality C can be maximized for an array of nanoslits [14].

These works have generated much interest in highly twisted fields [15] and a renewed interest in Lipkin’s zilch [8–11]. These ideas and results have been favorably accepted in the community, due to the simplicity and creativity as well as the possibility of greatly enhancing an inherently small measurement. Reference [2] has significant merit in that it looked at separating chiral properties of materials from the incident EM fields and was able to propose and implement an experiment that is theoretically and experimentally easy to understand and clear. It provided a way to creatively enhance the dissymmetry factor while giving physical meaning to the conserved quantities that Lipkin and colleagues once dismissed to be of little interest physically.

II. LIMITATIONS OF “SUPERCHIRAL” FIELDS

The heart of this paper is in showing explicitly the limitations of nodally enhanced optical enantioselectivity. Reference [3] briefly notes that the achiral $\chi|\mathbf{B}|^2$ response maintains the condition of $|g| \leq 2$ (which holds by definition), where χ represents the magnetic susceptibility. However, this magnetic term is never reinserted to correct the dissymmetry factor. Also, the dissymmetry factor enhancement $g/g_{\text{CPL}} = (1 + \sqrt{R})/(1 - \sqrt{R})$ shows no limit nor dependence on the material. The $\chi|\mathbf{B}|^2$ term was ignored, as commonly done, due to its typically small magnitude compared to the $\alpha|\mathbf{E}|^2$ term, where α is the electric polarizability. Due to the unlimited enhancement factor (albeit from a weakened signal), Tang and Cohen called such fields “superchiral”. (Since no limits have been placed on this enhancement factor, it is easy to think the enhancement can be arbitrarily large, as is implied by Eq. (5) [8]).

In Ref. [3], it is stated that a 400-fold enhancement may be possible with $R = 0.99$, or that a silver mirror with $R = 92\%$ may lead to a 48-fold enhancement in g_{max} . Hence, Ref. [2] stated that their chiral enhancement of ~ 10 –11 was not a fundamental limit. They continued that greater than a $10\times$ enhancement may be obtained at the expense of lower overall excitation rate simply by choosing a mirror with higher reflectivity.

By the Cauchy-Schwarz inequality, and by definition, the enhancement of the dissymmetry factor must be finite (see Appendix A). In this paper, we show that there is a fundamental limit to the enhancement, even with perfect measurement devices, and it is determined by the material chosen. We demonstrate this by showing that the $\chi|\mathbf{B}|^2$ response must be included consistently. This term is important, since the denominator in Eq. (2) should be related to the full EM field energy density, which is constant for a standing wave. In fact, Bliokh and Nori correctly stated that if U_e was replaced by the EM total energy density U_{total} , the ratio C/U_{total} would be bounded [8]. The final form of the dissymmetry factor in Ref. [3], where the enhancement comes from the denominator being U_e not U_{total} , was accepted as complete, however. We show that U_e should be replaced by $(U_e + \gamma U_b)$ in the dissymmetry factor, where γ is the weighting factor between the magnetic field energy density to electric field energy density.

Due to conservation of field energy, when U_e is minimum, U_b is maximum, and we can no longer ignore $\chi|\mathbf{B}|^2$. Usually

it is acceptable to ignore $\chi|\mathbf{B}|^2$ ($\ll \alpha|\mathbf{E}|^2$) but not at or near the node of the electric field energy. Typically electric dipole selection rules exclude the magnetic dipole transitions, but this is an approximation, and in reality the magnetic dipole terms still contribute [13,16,17]. “Dipole-forbidden” transitions occur with probabilities smaller by powers of $R_{\text{mol}}/\lambda \sim 1/1000$ than dipole-allowed transitions ($R_{\text{mol}} \sim 0.2\text{--}1$ nm is the size of the molecule) [13]. Since these transitions with the magnetic dipole term is used for the SWCF, it would be consistent to include this term in all equations.

In addition, the formalism reported earlier assumed C and the EM fields to be in vacuum, when in reality they are in a chiral medium that shows chiroptical effects, including ORD. We considered a chiral medium for C and EM fields. This allowed us to expand the definition of C and the derivation for g to linear medium instead of vacuum. We have included this generalization to be complete and to determine the effects of the chiral medium on the dissymmetry factor enhancement of opposite enantiomers.

In regards to the experiment by Hendry *et al.*, where an enhancement of 10^6 was observed, we note that only up to 10^2 factor was attributable to electric-magnetic dipolar interaction [18]. This is consistent with our model. The other four orders of magnitude appear to be from evanescent near-field modes [8] and is not included in our discussion because we focus on the far-field limit.

III. DISSYMMETRY FACTOR g DERIVATIONS: KEY POINTS

We now derive the generalized dissymmetry factor g for linear medium. Here we provide the key steps and results and leave other details to the appendixes. Initially, we follow Ref. [3] and also utilize Barron’s semiclassical perturbation model for chiroptical effects [1].

A. Assumptions

We assume isotropic linear medium. We also assume that there are no free charges or current densities, so that the multipole moments are induced from the incident EM fields only. We derive our equations for monochromatic EM fields, with angular frequency ω , noting that arbitrary fields may be Fourier transformed into linear combinations of monochromatic fields. We consider the change of chirality due to the EM fields, while the set of molecules being measured remains the same. Although the electric dipole moment $\mathbf{p} \rightarrow \pm\mathbf{p}$ from spatial inversion, since we are interested in the parity change of the EM fields, only $\mathbf{E} \rightarrow \pm\mathbf{E}$, since either the fields or the enantiomers change, not both, for a given measurement.

B. Induced dipole moments

Beginning with Barron’s induced multipole moments, we derive the complex induced electric ($\tilde{\mathbf{p}}$) and magnetic ($\tilde{\mathbf{m}}$) dipole moments (see Appendix B):

$$\tilde{\mathbf{p}} \simeq \tilde{\alpha}\tilde{\mathbf{E}} + \tilde{G}\tilde{\mathbf{B}}, \quad \tilde{\mathbf{m}} \simeq \tilde{\chi}\tilde{\mathbf{B}} - \tilde{G}\tilde{\mathbf{E}}. \quad (6)$$

Here, $\tilde{\mathbf{E}}$ and $\tilde{\mathbf{B}}$ are the complex electric and magnetic field vectors, respectively. The polarizability tensors all become scalars for an isotropic medium: $\tilde{\alpha}$ is the complex electric

polarizability, $\tilde{\chi}$ is the complex magnetic susceptibility, and \tilde{G} is the complex mixed electric-magnetic dipole polarizability. The electric-quadrupole moment averages to zero for isotropic samples and is not included here, even though it has the same magnitude as the magnetic dipole [19,20].

Quantities with a tilde are complex. For example, $\tilde{\alpha} = \alpha' + i\alpha''$, with $\alpha', \alpha'' \in \mathbb{R}$. To obtain the physical, that is, real, electric field vector \mathbf{E} , we simply take the real part of the complex field:

$$\mathbf{E} = \text{Re}\{\tilde{\mathbf{E}}\} = \frac{1}{2}(\tilde{\mathbf{E}} + \tilde{\mathbf{E}}^*). \quad (7)$$

Similarly, we can obtain the physical (real) \mathbf{B} , \mathbf{p} , and \mathbf{m} . It is important to be careful when obtaining physical quantities from the multiplication of complex quantities. In Eq. (6), we should take the real part of each side to obtain physical quantities.

Note that Eq. (6) is equivalent to Eq. (2) of Ref. [3]:

$$\tilde{\mathbf{p}} \simeq \tilde{\alpha}\tilde{\mathbf{E}} - i\tilde{G}_{\text{TC}}\tilde{\mathbf{B}}, \quad \tilde{\mathbf{m}} \simeq \tilde{\chi}\tilde{\mathbf{B}} + i\tilde{G}_{\text{TC}}\tilde{\mathbf{E}}, \quad (8)$$

where \tilde{G}_{TC} is the “ \tilde{G} ” used in Ref. [3].

In our paper, we follow Barron’s notations, together with notations from Ref. [3], which are consistent with each other for the most part. However, they differ in the mixed electric-magnetic dipole polarizability \tilde{G} , and we have chosen to use Barron’s notation for added clarity on the exact quantum multipole moments involved. The relationship between \tilde{G}_{TC} and our \tilde{G} is simply

$$\tilde{G} = -i\tilde{G}_{\text{TC}}. \quad (9)$$

What will be more useful is the relationship between the real and imaginary components of \tilde{G} :

$$\tilde{G} = G'(g) - iG'(f), \quad (10a)$$

$$\tilde{G}_{\text{TC}} = G'_{\text{TC}} + iG''_{\text{TC}}, \quad (10b)$$

with

$$G'(g) = \text{Re}\{\tilde{G}\} = G''_{\text{TC}} = \text{Im}\{G_{\text{TC}}\}, \quad (11a)$$

$$G'(f) = -\text{Im}\{\tilde{G}\} = G'_{\text{TC}} = \text{Re}\{G_{\text{TC}}\}. \quad (11b)$$

These relationships can be obtained from Eqs. (E26), (6), and (8).

To avoid confusion, it is important to note that here, G' does *not* denote the real part of \tilde{G} , as in $\tilde{\alpha} = \alpha' + i\alpha''$. For example, $G'(f)$ is not the real part of our G , although $G'(g)$ is. To avoid further confusion, we refrain from using G' , other than G'_{TC} , and instead use it with arguments only, for example, $G'(f)$, $G'(g)$. We have maintained this notation since it is the actual G' polarizability given in Ref. [1], where g and f inside the parentheses are the absorption and dispersion line-shape functions, respectively (Appendix C). The orientationally averaged isotropic molecular property terms $\tilde{\alpha}, \tilde{\chi}, \tilde{G}$ in Eq. (6) are derived in detail in Appendixes D and E.

C. Absorption rate, A^\pm

Work done by EM fields in the presence of electric and magnetic dipoles is

$$W_{\text{EM}} = \mathbf{p} \cdot \mathbf{E} + \mathbf{m} \cdot \mathbf{B}. \quad (12)$$

The rate of energy absorbed by such dipoles then is the sum of the rate of electric dipole absorption in electric field [$\mathbf{v} \cdot (\mathbf{Electric\ Force}) = \mathbf{v} \cdot (q\mathbf{E}) = \dot{\mathbf{p}} \cdot \mathbf{E}$] and the rate of magnetic dipole absorption of angular energy in the magnetic field ($\dot{\mathbf{m}} \cdot \mathbf{B}$).

So the total absorption rate of the molecules can be written as in Ref. [3]:

$$A^\pm = \langle \dot{\mathbf{p}} \cdot \mathbf{E} + \dot{\mathbf{m}} \cdot \mathbf{B} \rangle_t, \quad (13)$$

where the time average was taken ($\langle \dots \rangle_t$), since optical frequencies $\nu = c/\lambda \sim 10^{15}$ Hz are typically too fast to measure instantaneously. The (+) and (−) superscripts are for left-handed and right-handed EM fields, respectively, which come from spatial inversion, for which \mathbf{E} is odd and \mathbf{B} is even.

We use $e^{-i\omega t}$ harmonic time dependence (HTD), as used in Refs. [1] and [3], with general monochromatic complex EM fields and complex dipoles:

$$\tilde{\mathbf{E}}(t) = \pm \tilde{\mathbf{E}}_0 e^{-i\omega t}, \quad \tilde{\mathbf{B}}(t) = \tilde{\mathbf{B}}_0 e^{-i\omega t}, \quad (14a)$$

$$\tilde{\mathbf{p}}(t) = \tilde{\mathbf{p}}_0 e^{-i\omega t}, \quad \tilde{\mathbf{m}}(t) = \tilde{\mathbf{m}}_0 e^{-i\omega t}. \quad (14b)$$

To simplify our equations, we do not include the time dependence explicitly, but it should be remembered that these are time-dependent fields and induced dipoles. For a given set of molecules, we are interested in the parity change for the EM fields, so $\mathbf{E} \rightarrow \pm \mathbf{E}$.

We now substitute Eqs. (14) into Eq. (13), keeping in mind that the real parts of \mathbf{p} and \mathbf{m} must be taken, before multiplying to the real parts of \mathbf{E} and \mathbf{B} , respectively:

$$\begin{aligned} A^\pm &= \langle \dot{\mathbf{p}} \cdot \mathbf{E} + \dot{\mathbf{m}} \cdot \mathbf{B} \rangle_t \\ &= \frac{1}{4} \left\langle \frac{d(\tilde{\mathbf{p}} + \tilde{\mathbf{p}}^*)}{dt} \cdot (\tilde{\mathbf{E}} + \tilde{\mathbf{E}}^*) + \frac{d(\tilde{\mathbf{m}} + \tilde{\mathbf{m}}^*)}{dt} \cdot (\tilde{\mathbf{B}} + \tilde{\mathbf{B}}^*) \right\rangle_t \\ &= \frac{\omega}{2} \text{Im}(\tilde{\mathbf{p}} \cdot \tilde{\mathbf{E}}^* + \tilde{\mathbf{m}} \cdot \tilde{\mathbf{B}}^*). \end{aligned} \quad (15)$$

We can then substitute Eqs. (6) into Eq. (15) to arrive at a similar result as in Ref. [3]:

$$A^\pm \simeq (\alpha'' |\tilde{\mathbf{E}}|^2 + \chi'' |\tilde{\mathbf{B}}|^2) + G'(g) \omega \text{Im}[(\tilde{\mathbf{E}}^\pm)^* \cdot \tilde{\mathbf{B}}], \quad (16)$$

where we used $\text{Re}(\tilde{G}) = G'(g)$ from Eq. (11a).

We have included the \pm sign for odd parity of the \mathbf{E} field, in the last step. For a given enantiomer, this is where the CD sign change occurs. This is strictly true only for vacuum, as is shown in the next section. The molecular property terms α'' , χ'' , and $G'(g)$ are fixed for a given set of molecules.

D. Including generalized optical chirality C_g for linear media

So far, we have verified the results in Ref. [3]. The only approximation used was that the multipole moments used in Eqs. (6) and (13) were sufficient. We now begin to deviate from the theory in Ref. [3], and develop a more general theory from which the results from Ref. [3] can be derived under certain conditions. Using the results from Appendix F, we write A^\pm in terms of the generalized optical chirality C_g :

$$A^\pm \simeq \frac{\omega}{2} (\alpha'' |\tilde{\mathbf{E}}|^2 + \chi'' |\tilde{\mathbf{B}}|^2) - G'(g) \frac{2}{\epsilon} C_g^\pm, \quad (17)$$

where

$$C_g \equiv \frac{\epsilon}{2} \mathbf{E} \cdot (\nabla \times \mathbf{E}) + \frac{1}{2\mu} \mathbf{B} \cdot (\nabla \times \mathbf{B}). \quad (18)$$

This quantity is time-independent and valid for linear medium, with no free current or charges. Here it is worth mentioning that Cameron, Barnett, and Yao suggest that a “helicity density” should be used in lieu of the optical chirality (the Z^{000} zilch) since the former actually has the dimensions of angular momentum per unit volume [10,11]. Together with the fact that C_g is not a purely optical property for a linear medium, the term “optical chirality” may require some qualifications. However, since for monochromatic fields, the helicity densities and the zilches are simply proportional to one another by the square of the angular frequency, for our discussion we continue to use C_g and refer to it as the optical chirality.

We now consider our generalization of EM fields in a linear medium, not vacuum. This is done by realizing that for linear medium, due to ORD, the index of refraction may be (\pm)-dependent, which affects the relationship between \mathbf{E} and \mathbf{B} . This is due to n^L and n^R , the indices of refraction for LCPL and RCPL, respectively, being different and present. It is important to note that n^+ and n^- are not the same as n^R or n^L . This strictly depends on how we define the (\pm) configuration for our general EM field arrangement.

To clarify these points and for completeness, we note that C_g has a handedness included in it, as it is odd under parity because of the curl operator (or from the original \mathbf{E} field in the previous equations). The handedness of C_g also includes the effects from ORD. We thus include the following clarifying definition:

$$\begin{aligned} C_g^\pm &\equiv \left[\frac{\epsilon}{2} \mathbf{E} \cdot (\nabla \times \mathbf{E}) + \frac{1}{2\mu} \mathbf{B} \cdot (\nabla \times \mathbf{B}) \right]^\pm \\ &= \left[\frac{\epsilon^\pm}{2} \mathbf{E}^\pm \cdot (\nabla \times \mathbf{E})^\pm + \frac{1}{2\mu^\pm} \mathbf{B}^\pm \cdot (\nabla \times \mathbf{B})^\pm \right] \\ &\approx \pm \left[\frac{\epsilon^+}{2} \mathbf{E}^+ \cdot (\nabla \times \mathbf{E})^+ + \frac{1}{2\mu^+} \mathbf{B}^+ \cdot (\nabla \times \mathbf{B})^+ \right], \end{aligned} \quad (19)$$

where (+) superscript is for “left-handed” and (−) is for “right-handed.” For linear medium, the permittivity and permeability are different for oppositely handed EM fields, due to optical rotation; this is also why $\mathbf{B} \sim (n/c)\mathbf{E}$ was written with a (\pm) superscript above. The relationship between left-handed optical chirality (C_g^+) and right-handed optical chirality (C_g^-) is seen to be

$$C_g^+ \approx -C_g^-. \quad (20)$$

They are not equal because we are considering chiral media.

We then substitute Eq. (19) into Eq. (17) to rewrite the absorption rate as follows:

$$A^\pm \simeq A_a^\pm + A_c^\pm, \quad (21a)$$

where

$$A_a^\pm \equiv \omega \alpha'' \frac{2}{\epsilon^\pm} [\langle U_e \rangle_t^\pm + \gamma^\pm \langle U_b \rangle_t^\pm] \equiv \omega \alpha'' \frac{2}{\epsilon^\pm} U_\gamma^\pm, \quad (21b)$$

$$A_c^\pm \equiv -G'(g) \frac{2}{\epsilon^\pm} C_g^\pm, \quad (21c)$$

A_a^\pm, A_c^\pm being the ‘‘achiral’’ and ‘‘chiral’’ absorption rates, respectively (though neither is purely achiral nor chiral, precisely speaking), and

$$\gamma^\pm \equiv \frac{(n^\pm)^2 \chi''}{c^2 \alpha''} \geq 0. \quad (21d)$$

In Eq. (21b), the time averages of the electric field energy density (U_e) and the magnetic field energy density (U_b) are [21]

$$\langle U_e \rangle_t = \left\langle \frac{\epsilon}{2} |\mathbf{E}|^2 \right\rangle_t = \frac{\epsilon}{4} |\tilde{\mathbf{E}}|^2, \quad (22a)$$

$$\langle U_b \rangle_t = \left\langle \frac{1}{2\mu} |\mathbf{B}|^2 \right\rangle_t = \frac{1}{4\mu} |\tilde{\mathbf{B}}|^2. \quad (22b)$$

Equations (21) are one of the main results of this paper and are used to correctly derive the generalized dissymmetry factor g . The parameter γ is what limits the enhancement effect of the dissymmetry factor, as is shown later in Sec. IV E. From its definition, and from Eqs. (E9) and (E18), we see that for positive absorption line shape, this is a positive real quantity. For a second-order process, where higher-order processes such as stimulated emission are not involved, the absorption line-shape function g included in χ'' and α'' is positive for positive frequencies. Also, the range of γ is typically $\approx (10^{-6} - 10^{-4})$ as shown in Appendix G.

Equations (21) were written in this form to provide a somewhat more physically intuitive explanation of the various components involved than Eq. (17). We see from Eq. (21b) that the achiral contribution comes from a combination of EM field energy densities that is slightly different from the total EM field energy density. It is also dependent on the electric polarizability ($\alpha \sim |\mu|^2$ [Eq. (E9)]), which is typically the largest contribution to the achiral signal. From Eq. (21c), the chiral contribution is mainly dependent on the optical chirality C_g that, according to Ref. [3], determines the degree of chiral asymmetry in the rate of excitation for molecules. We also see that it is dependent on $G'(\sim \text{Im}(\langle \boldsymbol{\mu} \cdot \mathbf{m} \rangle))$ [Eq. (E28)], which is the main contribution to CD and ORD signals [1, 19].

Before ending this section, we provide the following equation for U_γ , obtained by comparing Eqs. (17) and (21b), which will be useful for future calculations:

$$\frac{2}{\epsilon^\pm} U_\gamma^\pm = \frac{1}{2} \left(|\tilde{\mathbf{E}}^\pm|^2 + \frac{\chi''}{\alpha''} |\tilde{\mathbf{B}}^\pm|^2 \right). \quad (23)$$

E. Generalized dissymmetry factor g

We substitute Eqs. (21) into the definition of the dissymmetry factor, g , given in Eq. (2):

$$\begin{aligned} g &\equiv \frac{A^+ - A^-}{\frac{1}{2}(A^+ + A^-)} \\ &\simeq \frac{\omega \alpha'' \left(\frac{2}{\epsilon^+} U_\gamma^+ - \frac{2}{\epsilon^-} U_\gamma^- \right) - G'(\mathbf{g}) \left(\frac{2}{\epsilon^+} C_g^+ - \frac{2}{\epsilon^-} C_g^- \right)}{\frac{1}{2} \left[\omega \alpha'' \left(\frac{2}{\epsilon^+} U_\gamma^+ + \frac{2}{\epsilon^-} U_\gamma^- \right) - G'(\mathbf{g}) \left(\frac{2}{\epsilon^+} C_g^+ + \frac{2}{\epsilon^-} C_g^- \right) \right]} \\ &= \frac{1}{2} g_{\text{CPL}} \left\{ \frac{g_{\text{CPL}} \left(\frac{2}{\epsilon^+} U_\gamma^+ - \frac{2}{\epsilon^-} U_\gamma^- \right) + \frac{c}{\omega n_{\text{ave}}^0} \left(\frac{2}{\epsilon^+} C_g^+ - \frac{2}{\epsilon^-} C_g^- \right)}{\left(\frac{2}{\epsilon^+} U_\gamma^+ + \frac{2}{\epsilon^-} U_\gamma^- \right) + \frac{g_{\text{CPL}}}{4} \frac{c}{\omega n_{\text{ave}}^0} \left(\frac{2}{\epsilon^+} C_g^+ + \frac{2}{\epsilon^-} C_g^- \right)} \right\}, \quad (24) \end{aligned}$$

where

$$n_{\text{ave}}^0 \equiv (n_{\text{ave}})_{\text{CPL}} = \frac{1}{2}(n^L + n^R) \quad (25)$$

is the average index of refraction for a dissymmetry factor measurement for CPL, since we include this in

$$g_{\text{CPL}} = -4 \frac{G'(\mathbf{g}) n_{\text{ave}}^0}{\alpha'' c}. \quad (26)$$

Equation (26) was obtained from Eq. (A1) [using Eqs. (B7a) and (B7f)], for an isotropic linear medium. The molecular property terms α'' and $G'(\mathbf{g})$, from Eqs. (E9) and (E28), were used since the dissymmetry factor was defined using the absorption rate.

It is worth noting that the CPL dissymmetry factor, g_{CPL} , is constant for a monochromatic field. Therefore, it only needs to be measured once to be used in the general dissymmetry factor g of Eq. (24). Equation (24) is the other main result of this paper. It is the general dissymmetry factor g for arbitrary EM fields in a linear medium.

For $n^+ \approx n^-$ or $n^L \approx n^R$:

$$\begin{aligned} \epsilon^\pm &\rightarrow \epsilon, & U_\gamma^\pm &\rightarrow U_\gamma, \\ \gamma^\pm &\rightarrow \gamma, & C_g^- &\rightarrow -C_g^+. \end{aligned} \quad (27)$$

We can then approximate the dissymmetry factor from Eq. (24) as

$$\begin{aligned} g &\approx \frac{1}{2} g_{\text{CPL}} \left\{ \frac{\frac{4}{g_{\text{CPL}}}(0) + \frac{c}{\omega n_{\text{ave}}^0} \frac{2}{\epsilon} [C_g^+ - (-C_g^+)]}{\frac{2}{\epsilon} (U_\gamma + U_\gamma) + \frac{g_{\text{CPL}}}{4} \frac{c}{\omega n_{\text{ave}}^0} (0)} \right\} \\ &= - \left(\frac{G'(\mathbf{g})}{\alpha''} \right) \left(\frac{2C_g^+}{\omega [\langle U_e \rangle_t + \gamma \langle U_b \rangle_t]} \right). \quad (28) \end{aligned}$$

This is a more physically intuitive equation than Eq. (24). Similar to the absorption rate A^\pm , from which it was derived, the dissymmetry factor signal g is increased when the chiral components G' and C_g , which are mainly composed of molecular and field properties, respectively, are increased. Likewise, the dissymmetry factor is decreased when the achiral components α'' and EM energy densities, composed mostly of molecular and field properties, respectively, are increased.

For $\gamma \rightarrow 0$ and EM fields in vacuum, as expected, this is reduced to the result in Ref. [3]:

$$g \rightarrow - \left(\frac{G''_{\text{TC}}}{\alpha''} \right) \left(\frac{2C}{\omega \langle U_e \rangle_t} \right). \quad (29)$$

We note that although this dissymmetry factor nicely separates the purely molecular property (G''_{TC}/α'') from the purely field property $(2C)/(\omega \langle U_e \rangle_t)$, this is, however, an approximation. It is not possible to separate the molecular properties in γ and C_g from the EM field properties in the generalized dissymmetry factor, as seen even in Eq. (28); the coupling is more complex for the general case in Eq. (24).

F. Application to dissymmetry factor for CPL

Now, let us verify the validity of Eq. (24) by considering the dissymmetry factor for CPL. Let us first change the (\pm)

notation for CPL. (+) \rightarrow (L) for LCPL and (-) \rightarrow (R) for RCPL. We first note that for CD measurements, to properly normalize,

$$|\mathbf{E}^L| = |\mathbf{E}^R| \equiv E. \quad (30)$$

From Eqs. (22a), (23), (H2), (H3b), and (H3c),

$$U_e^{(L/R)} \rightarrow \frac{\epsilon^{(L/R)}}{2} E^2, \quad (31a)$$

$$\frac{2}{\epsilon^{(L/R)}} U_\gamma^{(L/R)} \rightarrow \left(1 + \frac{\chi''}{\alpha''} \frac{(n^{(L/R)})^2}{c^2}\right) E^2. \quad (31b)$$

Using these, we first obtain the components

$$\left(\frac{2}{\epsilon^L} U_\gamma^L \mp \frac{2}{\epsilon^R} U_\gamma^R\right) = \left\{ (1 \mp 1) + \frac{\chi''}{\alpha'' c^2} [(n^L)^2 \mp (n^R)^2] \right\} E^2, \quad (32)$$

for g and obtain from Eq. (F5)

$$\left(\frac{2}{\epsilon^L} C_g^L \mp \frac{2}{\epsilon^R} C_g^R\right) = \frac{2\omega}{c} (n^L \pm n^R) E^2. \quad (33)$$

Now we combine all of this into Eq. (24):

$$\begin{aligned} g &\simeq \frac{1}{2} g_{\text{CPL}} \left\{ \frac{4}{g_{\text{CPL}}} \left(\frac{2}{\epsilon^L} U_\gamma^L - \frac{2}{\epsilon^R} U_\gamma^R \right) + \frac{c}{\omega n_{\text{ave}}^0} \left(\frac{2}{\epsilon^L} C_g^L - \frac{2}{\epsilon^R} C_g^R \right) \right\} \\ &= \frac{1}{2} g_{\text{CPL}} \left\{ \frac{4}{g_{\text{CPL}}} \gamma_{\text{ave}}^{\text{CPL}} \left[\frac{4n_{\text{ave}} \Delta n}{(n^2)_{\text{ave}}} \right] + 4 \right\} \\ &\approx 2g_{\text{CPL}} \left\{ \frac{4 \gamma_{\text{ave}}^{\text{CPL}} \left(\frac{\Delta n}{n_{\text{ave}}} \right) + 1}{2(1 + \gamma_{\text{ave}}^{\text{CPL}}) + g_{\text{CPL}} \frac{\Delta n}{n_{\text{ave}}}} \right\}, \quad (34) \end{aligned}$$

where

$$\gamma_{\text{ave}}^{\text{CPL}} \equiv \frac{\gamma^L + \gamma^R}{2} = \frac{(n^2)_{\text{ave}} \chi''}{c^2 \alpha''}, \quad (35a)$$

$$(n^2)_{\text{ave}} \equiv \frac{(n^L)^2 + (n^R)^2}{2}, \quad (35b)$$

$$n_{\text{ave}} \equiv \frac{n^L + n^R}{2}, \quad (35c)$$

$$\Delta n \equiv n^L - n_{\text{ave}} = \frac{n^L - n^R}{2}, \quad (35d)$$

$$\Delta n = n_{\text{ave}} - n^R. \quad (35e)$$

Note that $n_{\text{ave}} = n_{\text{ave}}^0$ was necessary to obtain the +1 term in the numerator for Eq. (34), so the n_{ave}^0 defined in Eq. (25) was the correct average index of refraction for g_{CPL} . Another subtlety is that $(n^2)_{\text{ave}} \neq (n_{\text{ave}})^2$, although it is a good approximation to say $(n^2)_{\text{ave}} \approx (n_{\text{ave}})^2$.

The orders of magnitude for the parameters in Eq. (34) are given in Appendix G and are summarized and adapted

below:

$$\gamma \simeq 10^{-6} - 10^{-4}, \quad (36a)$$

$$\Delta n/n \simeq 10^{-3} - 10^{-2}, \quad (36b)$$

$$g_{\text{CPL}} \simeq 10^{-3} - 10^{-2}, \quad (36c)$$

$$\frac{\gamma}{g_{\text{CPL}}} \frac{\Delta n}{n} \simeq 10^{-6} - 10^{-4} \simeq \gamma, \quad (36d)$$

$$g_{\text{CPL}} \frac{\Delta n}{n} \simeq 10^{-6} - 10^{-4} \simeq \gamma. \quad (36e)$$

Using Eqs. (36) in Eq. (34), we can see that parameters that are of order γ can be dropped when compared to order 1. Then,

$$g \rightarrow 2g_{\text{CPL}} \times \left\{ \frac{1}{2} \right\} = g_{\text{CPL}}. \quad \text{Q.E.D.} \quad (37)$$

We derived the dissymmetry factor for CPL using the full Eq. (24) to demonstrate that the details are correct in the equation. This was to show in detail where terms can be dropped and why, with accuracy. However, it could also be more easily derived from Eq. (28) using Eqs. (F5) and (H2):

$$\begin{aligned} g_{\text{CPL}} &\approx - \left(\frac{G'(\mathbf{g})}{\alpha''} \right) \left(\frac{2C_g^L}{\omega [\langle U_e \rangle_t + \gamma \langle U_b \rangle_t]_{\text{CPL}}} \right) \\ &= - \left(\frac{G'(\mathbf{g})}{\alpha''} \right) \left(\frac{4U_e n^L}{c U_e (1 + \gamma)} \right) \\ &\approx -4 \left(\frac{G'(\mathbf{g})}{\alpha''} \right) \left(\frac{n_{\text{ave}}}{c} \right). \quad \text{Q.E.D.} \quad (38) \end{aligned}$$

U_e is constant over time for CPL. We have also ignored $(\gamma \langle U_b \rangle_t = \gamma U_b)$ since it is smaller than U_e by $\gamma \approx (10^{-6} - 10^{-4})$. This is allowed here because U_b and U_e are equal and constant for a single CPL. As mentioned before, this is not always allowed, particularly for the standing wave case (SWCF).

IV. DISSYMMETRY FACTOR FOR STANDING WAVE CHIRAL FIELD

We now derive the dissymmetry factor for the SWCF arrangement in Refs. [2] and [3], where counterpropagating LCPL and RCPL generate a standing wave. We have assumed that the reflection at the mirror ($z = 0$ in Figs. 8 and 9 from Appendix H) occurs at normal incidence. Otherwise, polarization changes can occur with CPL becoming elliptically polarized (EP) [22]. We maintain the assumption in Refs. [2] and [3] that the boundary conditions of the chiral molecules may be ignored, despite the chiral material being thin and at a slight wedge angle.

A. Preparatory calculations

Much of the detail is contained in Appendix H. To calculate the dissymmetry factor in Eq. (24), we are interested in the

quantities

$$\left(\frac{2}{\epsilon^+} C_g^+ \mp \frac{2}{\epsilon^-} C_g^-\right), \quad \left(\frac{2}{\epsilon^+} U_\gamma^+ \mp \frac{2}{\epsilon^-} U_\gamma^-\right).$$

The former measures the difference or sum of the chirality of the EM fields for the two (\pm) SWCF arrangements. The latter measures the differential or total average absorption of the EM fields for these two arrangements.

From Eqs. (H9) and (H19), we have

$$\begin{aligned} & \left(\frac{2}{\epsilon^+} C_g^+ \mp \frac{2}{\epsilon^-} C_g^-\right) \\ &= -\frac{2\omega}{c} [-n^L (E_1^2 \mp E_2'^2) + n^R (E_2^2 \mp E_1'^2) \\ & \quad + (n^L - n^R)(E_1 E_2 \mp E_1' E_2') \cos(zk_{\text{tot}}z)]. \end{aligned} \quad (39)$$

Combining Eqs. (H13) and (H21), we obtain

$$\begin{aligned} & \left(\frac{2}{\epsilon^+} U_\gamma^+ \mp \frac{2}{\epsilon^-} U_\gamma^-\right) \\ &= \{[E_1^2 \mp (E_2')^2](1 + \gamma^L) + [E_2^2 \mp (E_1')^2](1 + \gamma^R) \\ & \quad + 2(E_1 E_2 \mp E_1' E_2')(\sqrt{\gamma^L \gamma^R} - 1) \cos(k_{\text{tot}}z)\}, \end{aligned} \quad (40)$$

where $E_1(E_1')$ and $E_2(E_2')$ are the amplitudes of the incident LCP (RCP) and reflected RCP (LCP) electric fields used to generate the SWCF.

B. Difference measurement scheme

For CD experiments, which is how the dissymmetry factor is measured, we can set the incident field amplitudes to be the same for (+) and (-) configurations. The irradiance (“intensity”) of the incident fields are matched, for proper normalization, during calibration. Inside a chiral medium, the irradiances of the EM fields are actually different, since energy depends on the permittivity and permeability of the material, which in turn depend on the handedness of the fields. However, the EM field irradiances are typically calibrated in an achiral medium, in which case matching the irradiances is equivalent to matching the field amplitudes. Hence, we can assume that the incident EM field amplitudes are equal.

Therefore,

$$|\mathbf{E}_1| = |\mathbf{E}_1'| = E_1, \quad (41)$$

from which it follows that

$$|\mathbf{E}_2| = |\mathbf{E}_2'| = E_2, \quad (42)$$

since the reflectivity is also the same:

$$R^{(+)} = R^{(-)} = R \equiv (E_2/E_1)^2. \quad (43)$$

We can then write Eq. (40) as

$$\left(\frac{2}{\epsilon^+} U_\gamma^+ - \frac{2}{\epsilon^-} U_\gamma^-\right) = (E_1^2 - E_2^2)[\gamma^L - \gamma^R], \quad (44a)$$

$$\begin{aligned} & \left(\frac{2}{\epsilon^+} U_\gamma^+ + \frac{2}{\epsilon^-} U_\gamma^-\right) = (E_1^2 + E_2^2)[2 + \gamma^L + \gamma^R] \\ & \quad + 4E_1 E_2(\sqrt{\gamma^L \gamma^R} - 1) \cos(k_{\text{tot}}z). \end{aligned} \quad (44b)$$

We can also write Eq. (39) as

$$\left(\frac{2}{\epsilon^+} C_g^+ - \frac{2}{\epsilon^-} C_g^-\right) = \frac{2\omega}{c} [(E_1^2 - E_2^2)(n^L + n^R)], \quad (45a)$$

and

$$\begin{aligned} & \left(\frac{2}{\epsilon^+} C_g^+ + \frac{2}{\epsilon^-} C_g^-\right) \\ &= \frac{2\omega}{c} (n^L - n^R)[E_1^2 + E_2^2 - 2E_1 E_2 \cos(zk_{\text{tot}}z)]. \end{aligned} \quad (45b)$$

C. Simplification using R and averaged parameters

Let us now write Eqs. (44) and (45) in terms of the reflectivity R . We substitute $\gamma_{\text{ave}}^{\text{CPL}}$, $(n^2)_{\text{ave}}$, k_{ave} , n_{ave}^0 , and Δn , using Eqs. (35a), (35b), (H12), (25), and (35d), respectively.

For U_γ ,

$$\begin{aligned} & \frac{1}{(E_1)^2} \left(\frac{2}{\epsilon^+} U_\gamma^+ - \frac{2}{\epsilon^-} U_\gamma^-\right) \\ &= 2(1 - R)\gamma_{\text{ave}}^{\text{CPL}} \left(\frac{2\Delta n}{n_{\text{ave}}^0}\right) \left[\frac{(n_{\text{ave}}^0)^2}{(n^2)_{\text{ave}}}\right], \end{aligned} \quad (46a)$$

and

$$\begin{aligned} & \frac{1}{(E_1)^2} \left(\frac{2}{\epsilon^+} U_\gamma^+ + \frac{2}{\epsilon^-} U_\gamma^-\right) \\ &= 2(1 + R)[1 + \gamma_{\text{ave}}^{\text{CPL}}] \\ & \quad + 4\sqrt{R} \left(\gamma_{\text{ave}}^{\text{CPL}} \frac{n^L n^R}{(n^2)_{\text{ave}}} - 1\right) (\cos[2k_{\text{ave}}z]). \end{aligned} \quad (46b)$$

For C_g ,

$$\frac{1}{(E_1)^2} \frac{1}{k_{\text{ave}}} \left(\frac{2}{\epsilon^+} C_g^+ - \frac{2}{\epsilon^-} C_g^-\right) = 4(1 - R) \quad (47a)$$

and

$$\begin{aligned} & \frac{1}{(E_1)^2} \frac{1}{k_{\text{ave}}} \left(\frac{2}{\epsilon^+} C_g^+ + \frac{2}{\epsilon^-} C_g^-\right) \\ &= 4 \left(\frac{\Delta n}{n_{\text{ave}}^0}\right) [1 + R - 2\sqrt{R}(\cos[2k_{\text{ave}}z])]. \end{aligned} \quad (47b)$$

D. Generalized dissymmetry factor g for SWCF

We finally substitute Eqs. (46) and (47) into the general formula, Eq. (24). The dissymmetry factor g for the standing wave formed by counterpropagating CPLs (SWCF) is then

$$g = \left\{ \frac{(1 - R)[4\gamma_{\text{ave}}^{\text{CPL}} \frac{n_{\text{ave}}^0 \Delta n}{(n^2)_{\text{ave}}} + g_{\text{CPL}}]}{(1 + R)[1 + \gamma_{\text{ave}}^{\text{CPL}} + \frac{1}{2}g_{\text{CPL}} \frac{\Delta n}{n_{\text{ave}}^0}] + 2\sqrt{R}[\gamma_{\text{ave}}^{\text{CPL}} \frac{n^L n^R}{(n^2)_{\text{ave}}} - 1 - \frac{1}{2}g_{\text{CPL}} \frac{\Delta n}{n_{\text{ave}}^0}] \cos(2k_{\text{ave}}z)} \right\}. \quad (48)$$

It is important to note that other than g_{CPL} or $\gamma_{\text{ave}}^{\text{CPL}}$, in Eq. (48), Δn and n_{ave}^0 always appear together as the ratio $(\Delta n/n_{\text{ave}}^0)$. g_{CPL} and $\gamma_{\text{ave}}^{\text{CPL}}$ can be obtained by measuring the CPL dissymmetry factor and g/g_{CPL} , while $(\Delta n/n_{\text{ave}}^0)$ can be obtained by measurement or by Kramers-Kronig transformation of the CD spectrum (see Appendix I). All three remain fixed for a given sample, independent of the EM fields.

We rewrite the parameters involved here, for convenience:

$$g_{\text{CPL}} = -4 \frac{G'(\mathbf{g})n_{\text{ave}}^0}{\alpha''c}, \quad (49a)$$

$$R \equiv (E_2/E_1)^2 = (E_2'/E_1')^2, \quad (49b)$$

$$\gamma_{\text{ave}}^{\text{CPL}} \equiv \frac{\gamma^L + \gamma^R}{2}, \quad (49c)$$

$$\gamma^{(L/R)} \equiv \frac{(n^{(L/R)})^2 \chi''}{c^2 \alpha''} \geq 0, \quad (49d)$$

$$n_{\text{ave}}^0 \equiv \frac{1}{2}(n^L + n^R), \quad (49e)$$

$$\Delta n \equiv \frac{n^L - n^R}{2} \quad (\Delta n : \text{positive or negative}), \quad (49f)$$

$$n^L = n_{\text{ave}}^0 + \Delta n, \quad (49g)$$

$$n^R = n_{\text{ave}}^0 - \Delta n, \quad (49h)$$

$$(n^2)_{\text{ave}} \equiv \frac{(n^L)^2 + (n^R)^2}{2}, \quad (49i)$$

$$k_{\text{ave}} \equiv \frac{k^L + k^R}{2} = \frac{\omega}{c} n_{\text{ave}}^0. \quad (49j)$$

Coles and Andrews recently derived a quantum electrodynamics version of the absorption rate difference [9]. Their analysis looked at the numerator term, that is, our $(A^+ - A^-)$, for counterpropagating beams. However, their A^+ and A^- were the absorption rates for the two oppositely handed enantiomers, not the difference between the two SWCF arrangements as measured in Ref. [2]. They also found terms with $(n^L - n^R)$ dependence, similar to our result, though they are for different contributions to the dissymmetry factor, since it is a different dissymmetry factor. They also have a shot noise term that is position-dependent, which they state corresponds to the nodal enhancement term seen in Refs. [2] and [3].

E. Simplified dissymmetry factor g_0 for $\Delta n = 0$

To gain a clearer understanding of the complicated dissymmetry factor in Eq. (48), we first simplify g for $\Delta n = 0$. This turns out to be a fairly good approximation to the full, generalized dissymmetry factor because $\Delta n/n_{\text{ave}}^0$ is typically very small.

When $\Delta n = 0$, we have the following relations from Eqs. (49):

$$n_0 \equiv n_{\text{ave}}^0 |_{(\Delta n=0)} = n^L = n^R, \quad (50a)$$

$$(n_0)^2 = (n^2)_{\text{ave}} |_{(\Delta n=0)}, \quad (50b)$$

$$\gamma_0 \equiv \gamma_{\text{ave}}^{\text{CPL}} |_{(\Delta n=0)} = \gamma^L = \gamma^R. \quad (50c)$$

Then Eq. (48) simplifies to

$$g_0 \equiv g(\Delta n/n_0 = 0) = g_{\text{CPL}} \times \left\{ \frac{(1-R)}{(1+R)(1+\gamma_0) + 2\sqrt{R}(\gamma_0-1)\cos(2k_{\text{ave}}z)} \right\}. \quad (51)$$

Equations (48) and (51) are the other main results of this paper, as both determine the characteristics and limitations of the SWCF-induced enantioselectivity measured in Ref. [2].

Note that we have kept the γ_0 terms, even though it is of order $\simeq(10^{-6}-10^{-4})$. Dropping the γ_0 terms can easily be thought to be valid, when compared to the 1 and -1 in Eq. (51). If these terms were dropped, we would obtain the same formula in Ref. [3], that is, Eq. (5). However, if we write the denominator in the form

$$\{[\langle U_e \rangle_t] + \gamma_0[\langle U_b \rangle_t]\} \propto [(1+R) - 2\sqrt{R}\cos(2k_{\text{ave}}z)] + \gamma_0[(1+R) + 2\sqrt{R}\cos(2k_{\text{ave}}z)], \quad (52)$$

we see that if we pick a position z such that $\langle U_e \rangle_t$ is a minimum, then $\langle U_b \rangle_t$ is at a maximum. Moreover, if we increase $R \rightarrow 1$, then $\langle U_e \rangle_t \rightarrow 0$ while $\langle U_b \rangle_t$ is both positive and finite. At this point, which is when the seemingly arbitrary enhancement of the SWCF occurs, the γ_0 (or, $\gamma_{\text{ave}}^{\text{CPL}}$) factor plays a nontrivial and crucial role. It limits the enhancement such that g/g_{CPL} remains finite, because the denominator now remains finite and away from zero. In fact, since the denominator remains finite though the numerator of Eq. (51) goes to zero, as $R \rightarrow 1$, the total enhancement $g/g_{\text{CPL}} \rightarrow 0$. Therefore, there is no enhancement after a certain point, as R gets closer to 1, contrary to Refs. [2] and [3].

Incidentally, we may ask when γ_0 matters. To simplify the discussion and to limit our point to that for maximum enhancement, we can answer this by looking at the nodal position of the electric field energy, that is, $\cos(2k_{\text{ave}}z) \rightarrow 1$. Then the denominator of Eq. (52) becomes

$$(1 - \sqrt{R})^2 + \gamma_0(1 + \sqrt{R})^2. \quad (53)$$

So γ_0 would matter when

$$(1 - \sqrt{R})^2 \approx \gamma_0(1 + \sqrt{R})^2, \quad (54)$$

or, equivalently, when

$$\sqrt{\gamma_0} = \frac{(1 - \sqrt{R})}{(1 + \sqrt{R})} \Leftrightarrow \sqrt{R} = \frac{(1 - \sqrt{\gamma_0})}{(1 + \sqrt{\gamma_0})}. \quad (55)$$

This is precisely when the maximum enhancement of g_0/g_{CPL} occurs, as is shown below.

V. STANDING WAVE CHIRAL FIELD: NUMERICAL SIMULATIONS

Here we analyze the generalized dissymmetry factor g in Eq. (48) for the SWCF arrangement obtained from counterpropagating LCPL and RCPL. For context and to apply our theory with physically relevant parameters, we use some of the parameter values derived from the experimental data in Ref. [2] for some of the plots and analyses.

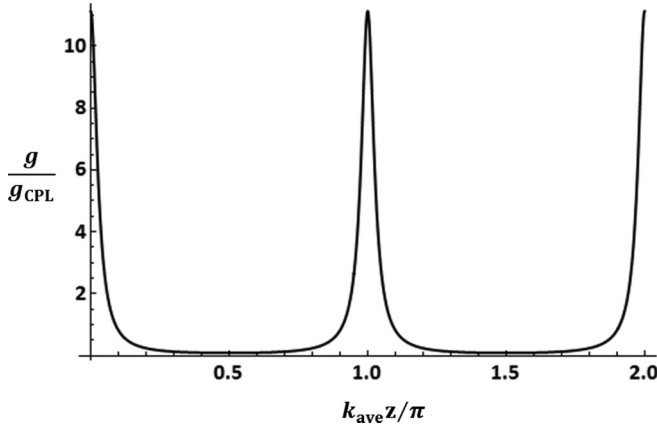


FIG. 1. Dissymmetry factor enhancement (g/g_{CPL}) for the standing wave (SWCF) arrangement, as a function of $(k_{\text{ave}}z/\pi)$. $R = 0.72$, $\Delta n/n_{\text{ave}}^0 = 0.00818$, and $\gamma_{\text{ave}}^{\text{CPL}} = 0.000781$. This plot shows that the maximum enhancement occurs when $k_{\text{ave}}z = l\pi$, where $l \in \mathbb{Z}$.

A. Standing wave position z for maximum g/g_{CPL}

Let us first determine the position z such that the dissymmetry factor enhancement g/g_{CPL} is maximum. From the simplified formula for g_0 in Eq. (51), it is obvious that the enhancement is maximized when $\cos(2k_{\text{ave}}z) \rightarrow 1$, for small γ_0 . This can also be seen in the full solution for g in Eq. (48), by recalling the orders of magnitude for the terms that multiply $\cos 2(k_{\text{ave}}z)$. For $\gamma_0 = 0.000781$, obtained by fitting to the measurements in Ref. [2], we can see graphically that this is the position that maximizes the enhancement (see Fig. 1).

B. Maximum dissymmetry enhancement g/g_{CPL} and corresponding R

For the case when $\Delta n/n_{\text{ave}}^0 = 0$, it is possible to obtain an analytical formula that is quite simple, for the maximum enhancement of the dissymmetry factor g_0/g_{CPL} . From the above section, we see that the maximum dissymmetry factor enhancement occurs when $\cos(2k_{\text{ave}}z) \rightarrow 1$. Then, using Eq. (51), it is easy to show that a quadratic equation remains when solving for an extremum. The enhancement has two extrema at $R = R_{\text{extrema}}^0$, where

$$\sqrt{R_{\text{extrema}}^0} = \frac{(1 \mp \sqrt{\gamma_0})^2}{(1 - \sqrt{\gamma_0})(1 + \sqrt{\gamma_0})}. \quad (56)$$

Since $(0 < \gamma_0 \ll 1)$ and $(R < 1)$ the physically valid R is that with $(\mp \rightarrow -)$ in the numerator. We can then conclude that g_0/g_{CPL} is maximized when $R = R_{\text{max}}^0$, where

$$R_{\text{max}}^0 = \left(\frac{1 - \sqrt{\gamma_0}}{1 + \sqrt{\gamma_0}} \right)^2. \quad (57)$$

Recall that this is the condition when γ_0 is large enough to contribute to the dissymmetry factor, as was seen in Eq. (55). The maximum enhancement for when $\Delta n/n_{\text{ave}}^0 = 0$ is then

$$\left(\frac{g_0}{g_{\text{CPL}}} \right)_{\text{max}} = \frac{1}{2\sqrt{\gamma_0}}. \quad (58)$$

Both Eqs. (57) and (58) are very good approximations for the general case for the physically valid range of values (see

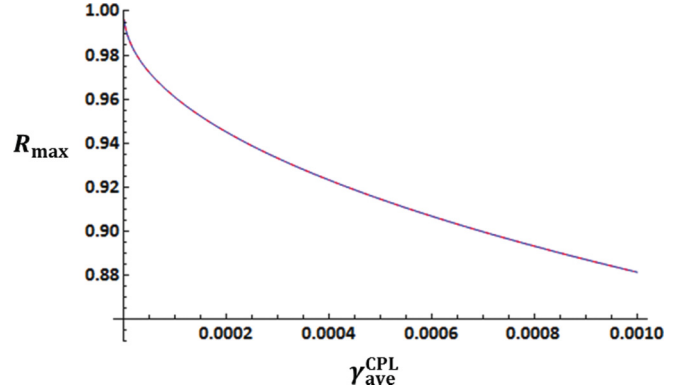


FIG. 2. (Color online) Reflectivity $R_{\text{max}}^0 = [(1 - \sqrt{\gamma})/(1 + \sqrt{\gamma})]^2$ and $R_{\text{max}}(\Delta n/n_{\text{ave}}^0 = 0.00818)$ for maximum enhancement g/g_{CPL} , for $\gamma_{\text{ave}}^{\text{CPL}} \in [10^{-6}, 10^{-3}]$. ($k_{\text{ave}}z$) set for U_e node. For R_{max} , $g_{\text{CPL}} = 1.42 \times 10^{-3}$. Both are indistinguishable here. Solid line, R_{max} ; dot-dashed line, $R_{\text{max}}^0(\gamma \rightarrow \gamma_{\text{ave}}^{\text{CPL}})$.

Appendix G) for g_{CPL} and $\Delta n/n_{\text{ave}}^0$. We will denote the general $(\Delta n/n_{\text{ave}}^0 \neq 0)$ R for maximum g/g_{CPL} as R_{max} . This was numerically solved and plotted in comparison to $R_{\text{max}}^0 = [(1 - \sqrt{\gamma_0})/(1 + \sqrt{\gamma_0})]^2|_{\gamma_0 \rightarrow \gamma_{\text{ave}}^{\text{CPL}}}$ in Fig. 2. We see that both agree quite well for the parameters given.

The maximum dissymmetry enhancement for the general case can be written as

$$\left(\frac{g}{g_{\text{CPL}}} \right)_{\text{max}} \approx \frac{1}{2\sqrt{\gamma_{\text{ave}}^{\text{CPL}}}}. \quad (59)$$

From Figs. 3 and 4, we can see that this is a good approximation to the actual maximum enhancement, the latter having been solved numerically.

We thus see that $\gamma = (n^2\chi'')/(c^2\alpha'')$ from Eq. (21d) is what determines the maximum dissymmetry enhancement g/g_{CPL} for all values of the reflectivity R . This enhancement can range from about 15 to 500, for physically reasonable values of γ . This implies that the enhancement effect is finite.

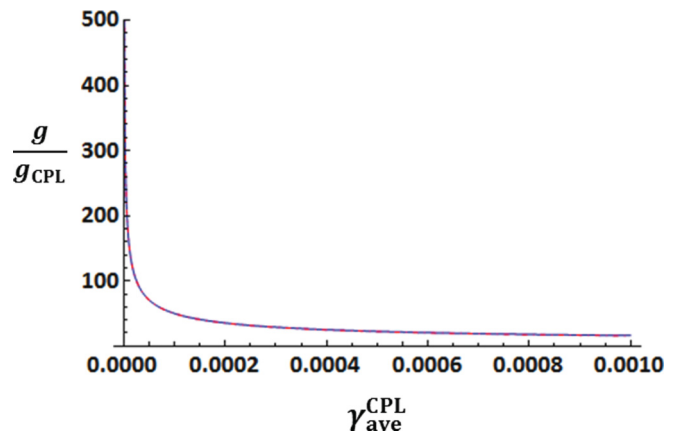


FIG. 3. (Color online) Maximum enhancement $g_0/g_{\text{CPL}} = 1/(2\sqrt{\gamma})$ and $g/g_{\text{CPL}}(\Delta n/n_{\text{ave}}^0 = 0.00818)$, for $\gamma_{\text{ave}}^{\text{CPL}} \in [10^{-6}, 10^{-3}]$. ($k_{\text{ave}}z$) set for U_e node. For g/g_{CPL} , $g_{\text{CPL}} = 1.42 \times 10^{-3}$. Both are indistinguishable here. Solid line, g/g_{CPL} ; dot-dashed line, $g_0/g_{\text{CPL}}(\gamma \rightarrow \gamma_{\text{ave}}^{\text{CPL}})$.

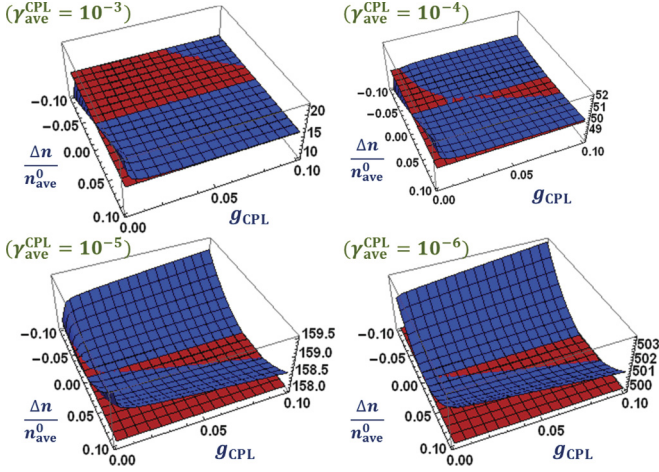


FIG. 4. (Color) Maximum enhancement $g_0/g_{CPL} = 1/(2\sqrt{\gamma})$ and $g/g_{CPL} (\Delta n \neq 0)$, for various γ_{ave}^{CPL} values. ($k_{ave}z$) set for U_e node. The plots provide the full range for g/g_{CPL} and show that both agree well. Curved blue plot, g/g_{CPL} ; constant red plot, $g_0/g_{CPL} (\gamma \rightarrow \gamma_{ave}^{CPL})$.

VI. APPLICATION TO TANG AND COHEN'S EXPERIMENT

A. Fit generalized g to experiment

We now apply our theory to the experiment in Ref. [2]. We first determine $(\Delta n/n_{ave}^0)$ from the m- and p-enantiomer CD measurements, via Kramers-Kronig transformation. This is done in Appendix I. With the approximation that $n_{ave}^0 \approx 1$, we use the average value between the two enantiomers in Eq. (I6c):

$$\frac{\Delta n}{n_{ave}^0} \rightarrow \Delta_0 = \pm 8.18 \times 10^{-3}, \quad (60)$$

where the positive $\Delta_0 (= +8.18 \times 10^{-3})$ is for the p-enantiomer and the negative $\Delta_0 (= -8.18 \times 10^{-3})$ is for the m-enantiomer, consistent with the ORD calculations seen in Fig. 10 in Appendix I, for the wavelength of the experiment.

The following measurements are for reflectivity $R = 0.72$ at $\lambda = 543.5$ nm wavelength, as reported in Ref. [2]:

$$(g_{max})_p = +1.50 \times 10^{-2} \pm 0.08 \times 10^{-2} \text{ (SEM)}, \quad (61a)$$

$$(g_{max})_m = -1.65 \times 10^{-2} \pm 0.08 \times 10^{-2} \text{ (SEM)}, \quad (61b)$$

$$(g_{CPL})_p = +1.41 \times 10^{-3} \pm 0.03 \times 10^{-3} \text{ (SEM)}, \quad (61c)$$

$$(g_{CPL})_m = -1.42 \times 10^{-3} \pm 0.04 \times 10^{-3} \text{ (SEM)}, \quad (61d)$$

$$(g/g_{CPL})_p = 10.6 \pm 0.6, \quad (61e)$$

$$(g/g_{CPL})_m = 11.6 \pm 0.6, \quad (61f)$$

where the m subscript is for the m-enantiomer, and the p subscript is for the p-enantiomer. Note that the g_{CPL} values are consistent with what we would expect from the order of magnitude estimation of Eq. (G5b).

From these measurements, we first take the averages of the enhancement factors and g_{CPL} :

$$\left(\frac{g}{g_{CPL}}\right)_{ave} = 11.1, \quad (62)$$

$$(g_{CPL})_{ave} = \pm 1.42 \times 10^{-3}, \quad (63)$$

where the positive $(g_{CPL})_{ave} (= +1.42 \times 10^{-3})$ is for the p-enantiomer and the negative $(g_{CPL})_{ave} (= -1.42 \times 10^{-3})$ is for the m-enantiomer.

We then set the following, in Eq. (48):

$$\frac{g}{g_{CPL}} \rightarrow \left(\frac{g}{g_{CPL}}\right)_{ave} = 11.1, \quad (64a)$$

$$g_{CPL} \rightarrow (g_{CPL})_{ave} = \pm 1.42 \times 10^{-3}, \quad (64b)$$

$$\frac{\Delta n}{n_{ave}^0} \rightarrow \Delta_0 = \pm 8.18 \times 10^{-3}, \quad (64c)$$

$$R \rightarrow 0.72, \quad (64d)$$

$$(k_{ave}z) \rightarrow l\pi \quad (l \in \mathbb{Z}). \quad (64e)$$

We can now fit for the experimental data to determine γ_{ave}^{CPL} . We numerically solve for γ_{ave}^{CPL} with Eqs. (64) substituted in Eq. (48). We obtained the following value:

$$\gamma_{ave}^{CPL} = 7.81 \times 10^{-4}. \quad (65)$$

This is consistent with our expected order-of-magnitude estimation in Eq. (G5a).

B. Symmetric g/g_{CPL} with respect to opposite enantiomers

For ideal enantiomers that are oppositely handed (such as the m- and p-enantiomers, if perfectly manufactured), the magnitudes of $\Delta n/n_{ave}^0$ (ORD) and g_{CPL} (from CD) are the same, but the signs are opposite. This can be seen to be the case from the measured g_{CPL} in Eqs. (61c) and (61d), as well as the ORD values in Eqs. (I6a) and (I6b).

However, the dissymmetry factors measured for the m- and p-enantiomers in Ref. [2] [Eqs. (61a) and (61b)], appear to have somewhat larger differences ($\sim 10\%$) than that for g_{CPL} ($\sim 0.7\%$) and $\Delta n/n_{ave}^0$ ($\sim 7\%$). We investigated whether this is from experimental errors, or whether one enantiomer would have preferential enhancement over the other, theoretically as well, in an SWCF.

We first analyze the dissymmetry factor g in Eq. (48). Opposite enantiomers have the following relations:

$$g_{CPL} \rightleftharpoons -g_{CPL}, \quad (66a)$$

$$\Delta n \rightleftharpoons -\Delta n, \quad (66b)$$

$$\gamma_{ave}^{CPL} \rightleftharpoons \gamma_{ave}^{CPL}, \quad (66c)$$

$$n_{ave}^0 \rightleftharpoons n_{ave}^0, \quad (66d)$$

$$n^L \rightleftharpoons n^R, \quad (66e)$$

$$(n^2)_{ave} \rightleftharpoons (n^2)_{ave}, \quad (66f)$$

$$k_{ave} \rightleftharpoons k_{ave}. \quad (66g)$$

With Eqs. (66), we see that the dissymmetry factor g in Eq. (48) has the same magnitude but opposite signs for opposite enantiomers. Then the enhancement, g/g_{CPL} is perfectly symmetric with respect to opposite enantiomers and should be identical.

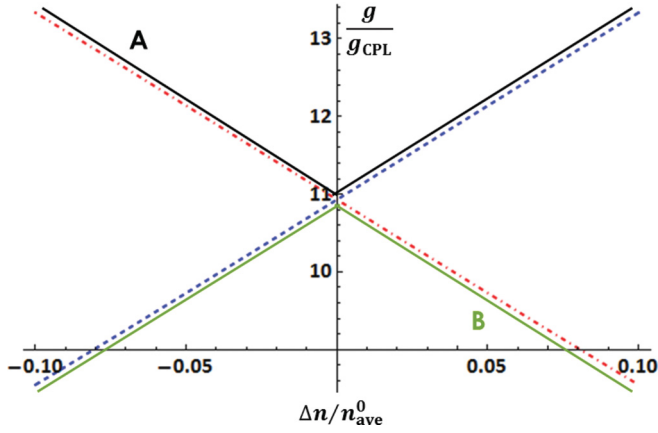


FIG. 5. (Color online) $\Delta n/n_{\text{ave}}^0 = (n^L - n^R)/(n^L + n^R)$ dependence of g/g_{CPL} for counterpropagating CPLs forming a standing wave (SWCF), for constant $g_{\text{CPL}} = \pm 1.42 \times 10^{-3}$. ($R = 0.72$, $\gamma_{\text{ave}}^{\text{CPL}} = 7.81 \times 10^{-4}$, $(k_{\text{ave}}z)$ set for U_e node.) Dashed line, positive $g_{\text{CPL}} = +1.42 \times 10^{-3}$; dot-dashed line, negative $g_{\text{CPL}} = -1.42 \times 10^{-3}$. For opposite enantiomers, both $\Delta n/n_{\text{ave}}^0$ and g_{CPL} change signs. So only the solid lines **A** and **B** are the physically valid curves, and only one is valid for a given frequency. Curve **A** corresponds to the experiment in Ref. [2].

We can also see this from Fig. 5. Each line (either dashed, with positive slope and positive g_{CPL} , or dot-dashed with negative slope and negative g_{CPL}) is a plot of the enhancement g/g_{CPL} as a function of $\Delta n/n_{\text{ave}}^0$. Since g_{CPL} also changes signs, when Δn changes signs, implying the enantiomer with opposite handedness is being measured instead, either the solid triangular line “**A**” or “**B**” is the allowed plot, not both, for a given incident light frequency. Curve **A** corresponds to the experimental region in Ref. [2], for the wavelength (543.5 nm) used. The kink at $\Delta n/n_{\text{ave}}^0 = 0$ is due to the fact that constant g_{CPL} was used, when in reality g_{CPL} should also vary along the graphs.

C. Generalized dissymmetry factor g vs reflectivity R

We conclude this section with the main plot that compares our theory and that in Refs. [2] and [3]. This is shown in Fig. 6, where the dissymmetry factor enhancement g/g_{CPL} is plotted against the reflectivity R . Here we see that there is a clear limit to the enhancement, which is fixed for the material used, and the enhancement goes to 0 when $R = 0$. We also see that both enantiomers have the same enhancement.

The maximum enhancement can be determined numerically from Eq. (48). For the experimental values in Ref. [2] ($g_{\text{CPL}} = 1.42 \times 10^{-3}$, $\gamma_{\text{ave}}^{\text{CPL}} = 7.81 \times 10^{-4}$, $\Delta n/n_{\text{ave}}^0 = 8.18 \times 10^{-3}$), the maximum enhancement $(g/g_{\text{CPL}})_{\text{max}} = 18.2$, which is obtained at $R_{\text{max}} = 0.894$. This matches the maximum for Fig. 6. This enhancement can also be approximated using Eq. (59), which is found to be 17.9.

VII. ADDITIONAL THOUGHTS

Though we have focused our analysis on the SWCF for counterpropagating CPLs, the limitations on the dissymmetry

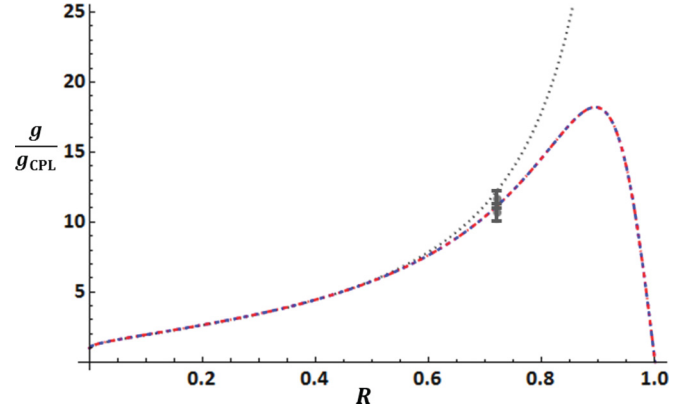


FIG. 6. (Color online) Comparison of $g(R)/g_{\text{CPL}}$ for our theory (dashed and dot-dashed lines) and that in Ref. [2] (dotted line) for the counterpropagating CPLs forming a SWCF. $g_{\text{CPL}} = \pm 1.42 \times 10^{-3}$, $\gamma_{\text{ave}}^{\text{CPL}} = 7.81 \times 10^{-4}$, $\Delta n/n_{\text{ave}}^0 = \pm 8.18 \times 10^{-3}$, $(k_{\text{ave}}z)$ set for U_e node. Positive g_{CPL} and $\Delta n/n_{\text{ave}}^0$ are used for p-enantiomer and negative values for m-enantiomer; the former is dashed line and the latter is dot-dashed line, but both are identical since both enantiomers should have same enhancement factor. The measured values and error bars for p (lower value) and m (higher value) from Ref. [2] are shown for $R = 0.72$.

factor enhancement is general. The limits should hold for any EM field that resonantly excites a molecular system. As we noted, $\gamma = (n^2 \chi'')/(c^2 \alpha'')$ in the mostly achiral term of the absorption rate, A_a , determines the balance between the time-averaged electric field energy density $\langle U_e \rangle_t$ and magnetic field energy density $\langle U_b \rangle_t$, as given in Eq. (21b):

$$A_a \equiv \omega \alpha'' \frac{2}{\epsilon} [\langle U_e \rangle_t + \gamma \langle U_b \rangle_t]. \quad (67)$$

Recall that it is when $\langle U_e \rangle_t \approx \gamma \langle U_b \rangle_t$ that the maximum enhancement occurred for the SWCF. The achiral A_a is present in the denominator for all dissymmetry factors that consider electric and magnetic dipole moments. So any enhancements that occur from nodal regions for the EM energy density should consider both $\langle U_e \rangle_t$ and $\gamma \langle U_b \rangle_t$ together, and hence would be limited by the parameter γ .

One might ask whether it is possible to set the magnetic field energy density to be 0 by eliminating the magnetic field **B** altogether. If the magnetic field component = 0 but the **E** field is not, then the arbitrarily large enhancement might be obtained as given in Eq. (5). We can answer this by recalling that magnetic fields may be absent only for a static (dc) electric field, according to the Maxwell equations. However, a static field cannot generate any absorption [1]. Hence, by conservation of EM field energy, the dissymmetry factor will always be limited in its nodal enhancement because both terms in Eq. (67) should always be present.

Another common question might be whether a material with γ arbitrarily small could be used, so that Eq. (5) might be applicable, or that the enhancement might be increased according to Eq. (59). Recall that the numerator of the dissymmetry factor in Eq. (24), from which the actual enantioselective *signal* emerges, is dependent on $G'(g)$. From

Eq. (E28), $G'(g) \sim \boldsymbol{\mu} \cdot \mathbf{m}$ and from Eq. (E18), $\chi'' \sim \mathbf{m} \cdot \mathbf{m}$. Thus, if $\gamma = (n^2 \chi'') / (c^2 \alpha'') \rightarrow 0$, then $G'(g) \rightarrow 0$ also, and the very signal that needs to be enhanced disappears.

In fact, it is important to realize that the very enhancement seen in the standing wave case comes at the expense of a decreased EM field energy to induce the enantioselective moments. We can see the signal decrease by looking at the denominator of the dissymmetry factor. For simplicity, since the same conclusions can be arrived for the generalized g for SWCF in Eq. (48), we use g_0 instead from Eq. (51). Since the *signal* for the SWCF experiment is directly from fluorescence, which, in turn, is proportional to the absorption, the signal of interest is the average absorption, that is, the denominator of the dissymmetry factor. This denominator is then given in Eq. (53) as $(1 - \sqrt{R})^2 + \gamma_0(1 + \sqrt{R})^2$. Recall that at the maximum enhancement, Eq. (54) holds, such that

$$\text{Denominator of } g_0 \rightarrow 2\gamma_0(1 + \sqrt{R_{\max}^0})^2 \approx 8\gamma_0. \quad (68)$$

So the signal is proportional to γ_0 . The enhancement of g/g_{CPL} , on the other hand, is proportional to $1/(2\sqrt{\gamma_0})$, according to Eq. (59). Then to compare the *decrease* in signal (as $\gamma_0 \rightarrow 0$) to the *increase* in enhancement, we compare with the *inverse* of (g/g_{CPL}) :

$$\frac{\text{Ave. signal}}{1/(g/g_{\text{CPL}})} \approx 4\sqrt{\gamma_0} \rightarrow 0 \quad \text{as } \gamma_0 \rightarrow 0. \quad (69)$$

This shows that the signal decreases faster than the increase in dissymmetry enhancement when searching for molecules with small γ .

Figure 7 shows the relationship between fluorescent signal and various γ values, for the nodal U_e position of the SWCF. Recall from Fig. 2 that the maximum g/g_{CPL} enhancement occurs around $R = 0.85$ – 1.0 . Then we can look at the values for the denominator of g_0 near $R = 0.85$ – 1.0 to determine

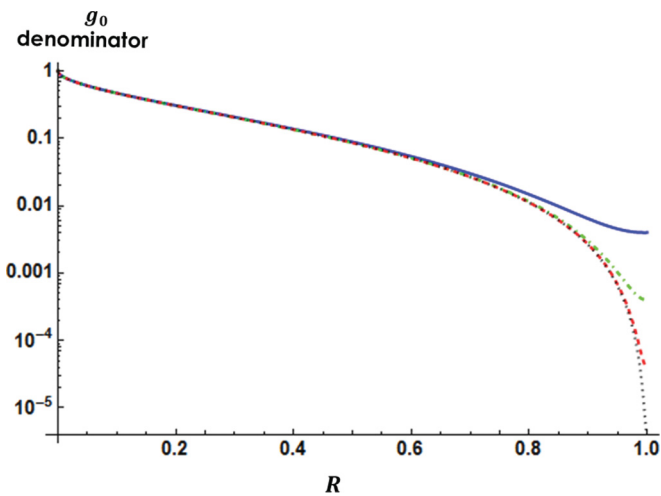


FIG. 7. (Color online) Log plot of the denominator of g_0 at the nodal U_e position for the SWCF. A decrease in $\gamma_{\text{ave}}^{\text{CPL}}$ corresponds to a decrease in the fluorescent signal by the same amount, as seen by values where the maximum enhancement occurs ($R \approx 0.85$ – 1.0). Solid line, $\gamma_{\text{ave}}^{\text{CPL}} = 10^{-3}$; dot-dashed line, $\gamma_{\text{ave}}^{\text{CPL}} = 10^{-4}$; dashed line, $\gamma_{\text{ave}}^{\text{CPL}} = 10^{-5}$; dotted line, $\gamma_{\text{ave}}^{\text{CPL}} = 10^{-6}$.

the region when the maximum dissymmetry enhancement occurs. We see that an order of magnitude decrease in $\gamma_{\text{ave}}^{\text{CPL}}$ corresponds to an order of magnitude decrease in the fluorescent signal itself. However, from Fig. 4, an order of magnitude of decrease in $\gamma_{\text{ave}}^{\text{CPL}}$ corresponds to a $\sqrt{10} \approx 3 \times$ increase in the enhancement (g/g_{CPL}). So finding a material with small $\gamma_{\text{ave}}^{\text{CPL}}$ eventually becomes fruitless since the signal itself will disappear faster than the enhancement.

One last point we include is that the equations derived for the SWCF can be generalized to elliptically polarized light (EPL). However, it can be shown that for EPLs, it is CPL that maximizes the dissymmetry factor enhancement. Thus, we have not included the EPL formalism in this paper.

VIII. ANALOGY BETWEEN ELLIPSOMETRIC CHIROPTICAL SPECTROSCOPY AND ENHANCED OPTICAL ENANTIOSELECTIVITY

In chiroptical spectroscopy, there have been a number of experimental schemes aimed at enhancing the sensitivity of the chiral characterization. One of the most successful schemes is based on the quasinull ellipsometry measurement technique developed by Kliger and co-workers [23,24]. Recently, this method was used by Helbing and Bonmarin [25] to measure the enhanced vibrational CD spectrum. We also showed that this ellipsometry measurement scheme with a supercontinuum pulse, whose spectrum covers almost the entire visible frequency region, can be used to obtain the electronic CD spectra of transition metal chiral molecules and J-aggregates of cyanine dyes bound to DNA [26]. Here, left- and right-EPL fields with their major axes in the x direction, that is, zero azimuth angle, interact with a chiral sample. By using a high-quality polarizer placed after the sample, only the intensity of the y component of the transmitted field is selectively measured. Then, the experimentally measured dissymmetry factor in this case is defined as [24]

$$g_{\text{EP},y} = \frac{I_{\text{LEP},y} - I_{\text{REP},y}}{(I_{\text{LEP},y} + I_{\text{REP},y})/2}. \quad (70)$$

Using either the Jones matrix formalism or linear response theory, one can show that the above dissymmetry factor is approximately given by

$$\begin{aligned} g_{\text{EP},y} &\propto \varepsilon \left(\frac{4 \text{Im}(\boldsymbol{\mu}_{eg} \cdot \mathbf{m}_{eg})}{|\boldsymbol{\mu}_{eg}|^2} \right) \left(\frac{E_y E_x}{E_y^2} \right) \\ &= \varepsilon \left(\frac{4 \text{Im}(\boldsymbol{\mu}_{eg} \cdot \mathbf{m}_{eg})}{|\boldsymbol{\mu}_{eg}|^2} \right) \left(\frac{1+r}{1-r} \right), \end{aligned} \quad (71)$$

where ε is the decadic molar extinction coefficient. Here, $E_x (= |\mathbf{E}_{\text{EPL}}| \cos \eta)$ and $E_y (= |\mathbf{E}_{\text{EPL}}| \sin \eta)$ are the electric field amplitudes of the x and y components of the incident EPL, and r in Eq. (71) is related to the ellipticity angle η as $\eta = \arctan(1-r)/(1+r)$.

From Eq. (71), as the ellipticity angle η is decreased to make the EPL closer to a linearly polarized light with polarization direction parallel to the x axis, the dissymmetry factor given in Eq. (71) can be dramatically enhanced. The enhancement factor $(1+r)/(1-r)$ in Eq. (71) is similar to that in Eq. (10) for the SWCF in Ref. [3] [our Eq. (5)]. Over the years, it has

been experimentally demonstrated that an order of magnitude enhancement of $g_{EP,y}$ can be easily achieved [26]. In fact, the underlying physics of this enhancement of the chiroptical measurement sensitivity is quite similar to that of the enhancement found in the SWCF-induced enantioselectivity in narrow regions of space. As the ellipticity angle η decreases, the intensity of the electric field along the y axis, which is the denominator in Eq. (71), decreases by $\sin^2 \eta$, which is analogous to the decrease of the electric field energy density $[(E_1 - E_2)^2]$ at the nodes of the SWCF as E_2 approaches E_1 . The numerator in Eq. (71) describes the mixed electric and magnetic dipole interactions with electric and magnetic fields, respectively. As the ellipticity angle decreases, even though the amplitude of the y component of the electric field decreases by $\sin \eta$, that of the y component of the magnetic field increases by $\cos \eta$. The numerator in Eq. (71) is thus proportional to $\sin \eta \cos \eta$, which is analogous to the decrease of the optical chirality $C_g[\propto(E_1 - E_2)(E_1 + E_2) = (1 - R)]$ that appears in the numerator of the dissymmetry factor g in Eq. (51). In experiments, however, such a limiting case where η approaches zero is not of interest at all, because the detected signal intensities, both $I_{LEP,y}$ and $I_{REP,y}$, become extremely small in this case and the signal-to-noise ratio (SNR) is deteriorated. Thus, experimentalists have tried to balance the chiral spectroscopic enhancement against the signal-to-noise diminution, carefully controlling the eccentricity of the left-and/or right-EPLs, depending on the specific detection scheme used.

In the quasinull ellipsometry for chiroptical spectroscopy, since the y component of the EPL is used as the intrinsic (phase-fixed) local oscillator (LO) field that interferes with the chiral signal field generated by the stronger E_x component of the incident EPL, this ellipsometric method has thus been known as a *self*-heterodyne detection method [25–27]. Instead of using the LO field inherently present in the incident EPL, one can use an independent linearly polarized LO whose polarization direction is parallel to the chiral signal field (the y component of the resulting free-induction-decay field) to enhance the interference signal intensity in an arbitrary manner [28,29], where a Mach-Zehnder type interferometry is employed for a phase-and-amplitude-sensitive detection of the chiral signal field [30]. Such spectroscopic enhancement effects were shown to be experimentally measurable and the so-called *active* heterodyne-detection method was used to amplify extremely weak infrared CD ($g_{CD} \approx 10^{-5}$) and ORD signals for small organic chiral molecules in solutions [28,31–34].

IX. CONCLUSION

The origin behind the enhancement of the chiral asymmetry, in the rate of excitation with locally enhanced chiral field, is quite similar to that of the characterization of molecular chirality, using either self- or active-heterodyne-detection method. However, the former, employing a SWCF, can be used to enhance the enantioselectivity in the excitation of certain enantiomers that are localized in the nodal regions of the field, but the latter cannot. Nonetheless, due to EM energy conservation and the fact that the EM total energy density is constant in the medium, there should be an upper limit of the

optical enantioselectivity that is generally set by the positivity of the rate of excitation and the Cauchy-Schwarz inequality.

Furthermore, we have shown that the chiral asymmetry in the rate of excitation cannot always be written as a product of material chirality and optical chirality. We have provided analysis for the molecular property tensors involved to quantify the dissymmetry factor enhancements. This should provide a guide to future studies on locally enhanced chiral fields. We anticipate that further investigation searching for locally enhanced chiral field in the vicinity of complex boundaries would be highly interesting in hopes of finding a way to enhance optical enantioselectivity in inhomogeneous catalysis employing surface plasmonics technology.

ACKNOWLEDGMENTS

This work was supported by NRF (Grants No. 2011-0020033 and No. 2009-0078897) and KBSI (Grant No. T32401) grants to M.C. J.S.C was supported by an IGERT Fellowship from the National Science Foundation.

APPENDIX A: PROPERTIES OF THE DISSYMMETRY FACTOR

An important result that is derived in Ref. [1] is the dissymmetry factor for CPL, in an isotropic medium. After orientational averaging, the dissymmetry factor for an isotropic sample can be written in terms of molecular transition moments (SI units):

$$g_{\text{CPL}}(j \leftarrow n) = \frac{4R(j \leftarrow n)}{cD(j \leftarrow n)}, \quad (\text{A1})$$

where

$$R(j \leftarrow n) = \text{Im}(\langle n|\mu|j\rangle\langle j|m|n\rangle), \quad (\text{A2})$$

$$D(j \leftarrow n) = \text{Re}(\langle n|\mu|j\rangle\langle j|\mu|n\rangle) \quad (\text{A3})$$

are the rotational strength and dipole strength of the $j \leftarrow n$ transition, respectively.

Also, by definition, the magnitude of the dissymmetry factor is bounded. The Cauchy-Schwarz inequality requires that the dissymmetry factor must be ≤ 2 in magnitude:

$$|g| = \left| 2 \frac{A^L - A^R}{A^L + A^R} \right| \leq 2 |A^L - A^R| \left| \frac{1}{A^L + A^R} \right| \leq 2. \quad (\text{A4})$$

We used the fact that the largest magnitude for the dissymmetry factor is obtained when $A^L = 0$ and $A^R \neq 0$ or vice versa.

APPENDIX B: DERIVATION OF \mathbf{p} AND \mathbf{m} MULTIPOLE EXPANSIONS

We derive Eq. (6) from the semiclassical perturbative formulation in Ref. [1]:

$$\tilde{\mathbf{p}} \simeq \tilde{\alpha} \tilde{\mathbf{E}} + \tilde{G} \tilde{\mathbf{B}}, \quad (\text{B1})$$

$$\tilde{\mathbf{m}} \simeq \tilde{\chi} \tilde{\mathbf{B}} - \tilde{G} \tilde{\mathbf{E}}. \quad (\text{B2})$$

Note that Ref. [1] uses “ μ ” for the electric dipole moment, whereas “ p ” is used in Ref. [3]. In this paper, μ and p are the same and used together.

We begin with the induced oscillating electric and magnetic multipole moments of molecules in a complex monochromatic EM field oscillating at angular frequency ω . This was obtained from applying perturbation theory to the Schrödinger equation:

$$\tilde{\mu}_\alpha = \tilde{\alpha}_{\alpha\beta}(\tilde{E}_\beta)_0 + \frac{1}{3}\tilde{A}_{\alpha,\beta\gamma}(\tilde{E}_{\beta\gamma})_0 + \tilde{G}_{\alpha\beta}(\tilde{B}_\beta)_0 + \dots, \quad (\text{B3})$$

$$\tilde{m}'_\alpha = \tilde{\chi}_{\alpha\beta}(\tilde{B}_\beta)_0 + \tilde{\mathcal{G}}_{\alpha\beta}(\tilde{E}_\beta)_0 + \frac{1}{3}\tilde{D}_{\alpha,\beta\gamma}(\tilde{E}_{\beta\gamma})_0 + \dots. \quad (\text{B4})$$

It is important to be careful when obtaining physical quantities from complex EM equations, particularly if there are complex quantities that are multiplied. Typically, the real parts of complex quantities are taken *before* multiplication, such as in

$$\mathbf{p} \cdot \mathbf{E} = [\text{Re}(\tilde{\mathbf{p}})] \cdot [\text{Re}(\tilde{\mathbf{E}})] = \left[\frac{1}{2}(\tilde{\mathbf{p}} + \tilde{\mathbf{p}}^*)\right] \cdot \left[\frac{1}{2}(\tilde{\mathbf{E}} + \tilde{\mathbf{E}}^*)\right].$$

However, in the formalism provided here, the multipole moments were constructed explicitly with complex EM fields and complex molecular property tensors, so complex multiplication has been carefully considered already. To obtain the actual physical multipole moment, μ_α or m'_α , which are the *real* parts of their complex versions in Eqs. (B3) and (B4), we simply take the real parts of the full formulas on the right-hand side of each equation:

$$\mu_\alpha = \text{Re}\left[\tilde{\alpha}_{\alpha\beta}(\tilde{E}_\beta)_0 + \frac{1}{3}\tilde{A}_{\alpha,\beta\gamma}(\tilde{E}_{\beta\gamma})_0 + \tilde{G}_{\alpha\beta}(\tilde{B}_\beta)_0 + \dots\right], \quad (\text{B5})$$

$$m'_\alpha = \text{Re}\left[\tilde{\chi}_{\alpha\beta}(\tilde{B}_\beta)_0 + \tilde{\mathcal{G}}_{\alpha\beta}(\tilde{E}_\beta)_0 + \frac{1}{3}\tilde{D}_{\alpha,\beta\gamma}(\tilde{E}_{\beta\gamma})_0 + \dots\right]. \quad (\text{B6})$$

In the above equations, \tilde{E}_β is the Cartesian component of the complex electric field vector, where $\beta = x, y, z$, and similarly for the magnetic field \tilde{B} ; $\tilde{\alpha}$ is the complex electric polarizability, $\tilde{\chi}$ is the complex magnetic susceptibility, and \tilde{G} is the complex mixed electric-magnetic dipole polarizability; \tilde{m}' is the magnetic dipole moment, including the diamagnetic contribution, which is the same as our \tilde{m} in Eq. (B2); $E_{\alpha\beta} \equiv \nabla_\alpha E_\beta$, and $(\mathbf{E})_0$ means that the field is taken at the molecular origin.

Before we can define the complex dynamic molecular property tensors given in Eqs. (B3) and (B4), we must first define the real dynamic molecular property tensors:

$$\alpha_{\alpha\beta} = \frac{2}{\hbar} \sum_{j \neq n} \frac{\omega_{jn}}{\omega_{jn}^2 - \omega^2} \text{Re}(\langle n | \mu_\alpha | j \rangle \langle j | \mu_\beta | n \rangle), \quad (\text{B7a})$$

$$\alpha'_{\alpha\beta} = -\frac{2}{\hbar} \sum_{j \neq n} \frac{\omega}{\omega_{jn}^2 - \omega^2} \text{Im}(\langle n | \mu_\alpha | j \rangle \langle j | \mu_\beta | n \rangle), \quad (\text{B7b})$$

$$A_{\alpha,\beta\gamma} = \frac{2}{\hbar} \sum_{j \neq n} \frac{\omega_{jn}}{\omega_{jn}^2 - \omega^2} \text{Re}(\langle n | \mu_\alpha | j \rangle \langle j | \Theta_{\beta\gamma} | n \rangle), \quad (\text{B7c})$$

$$A'_{\alpha,\beta\gamma} = -\frac{2}{\hbar} \sum_{j \neq n} \frac{\omega}{\omega_{jn}^2 - \omega^2} \text{Im}(\langle n | \mu_\alpha | j \rangle \langle j | \Theta_{\beta\gamma} | n \rangle), \quad (\text{B7d})$$

$$G_{\alpha\beta} = \frac{2}{\hbar} \sum_{j \neq n} \frac{\omega_{jn}}{\omega_{jn}^2 - \omega^2} \text{Re}(\langle n | \mu_\alpha | j \rangle \langle j | m_\beta | n \rangle), \quad (\text{B7e})$$

$$G'_{\alpha\beta} = -\frac{2}{\hbar} \sum_{j \neq n} \frac{\omega}{\omega_{jn}^2 - \omega^2} \text{Im}(\langle n | \mu_\alpha | j \rangle \langle j | m_\beta | n \rangle), \quad (\text{B7f})$$

$$D_{\alpha,\beta\gamma} = \frac{2}{\hbar} \sum_{j \neq n} \frac{\omega_{jn}}{\omega_{jn}^2 - \omega^2} \text{Re}(\langle n | m_\alpha | j \rangle \langle j | \Theta_{\beta\gamma} | n \rangle), \quad (\text{B7g})$$

$$D'_{\alpha,\beta\gamma} = -\frac{2}{\hbar} \sum_{j \neq n} \frac{\omega}{\omega_{jn}^2 - \omega^2} \text{Im}(\langle n | m_\alpha | j \rangle \langle j | \Theta_{\beta\gamma} | n \rangle), \quad (\text{B7h})$$

$$\begin{aligned} \chi_{\alpha\beta} &= \frac{2}{\hbar} \sum_{j \neq n} \frac{\omega_{jn}}{\omega_{jn}^2 - \omega^2} \text{Re}(\langle n | m_\alpha | j \rangle \langle j | m_\beta | n \rangle) \\ &\quad + \sum_i \frac{e_i^2}{4m_i} \langle n | r_{i\alpha} r_{i\beta} - r_i^2 \delta_{\alpha\beta} | n \rangle, \end{aligned} \quad (\text{B7i})$$

$$\chi'_{\alpha\beta} = -\frac{2}{\hbar} \sum_{j \neq n} \frac{\omega}{\omega_{jn}^2 - \omega^2} \text{Im}(\langle n | m_\alpha | j \rangle \langle j | m_\beta | n \rangle). \quad (\text{B7j})$$

Here, the sum is over the index j ; μ_α , m_α , $\Theta_{\alpha\beta}$ are the electric dipole, magnetic dipole, and electric quadrupole operators, respectively; $|j\rangle, |n\rangle$ are j th and n th unperturbed eigenfunction states; $\omega_{jn} = \omega_j - \omega_n$ and $\hbar\omega_j = E_j$ is the eigenvalue of the unperturbed molecular Hamiltonian H for the j th eigenstate; m_i is the mass of the i th charge, and e_i is its charge. Thus, the dynamic molecular property tensors are sums of transitions $j \leftarrow n$. Equations (B7) are given in Ref. [1] and are provided here for the sake of completeness.

The *complex* (with tilde) dynamic molecular property tensors given in Eqs. (B3) and (B4) are then defined in terms of their real counterparts:

$$\tilde{\alpha}_{\alpha\beta} = \alpha_{\alpha\beta} - i\alpha'_{\alpha\beta}, \quad (\text{B8})$$

and similarly for $\tilde{A}_{\alpha,\beta\gamma}$, $\tilde{G}_{\alpha\beta}$, $\tilde{D}_{\alpha,\beta\gamma}$, and $\tilde{\chi}_{\alpha\beta}$.

A small adjustment is made for $\tilde{\mathcal{G}}_{\alpha\beta}$ to properly account for the absorption of fields and the multiplication of complex quantities:

$$\begin{aligned} \tilde{\mathcal{G}}_{\alpha\beta} &= \frac{2}{\hbar} \sum_{j \neq n} \frac{1}{\omega_{jn}^2 - \omega^2} [\omega_{jn} \text{Re}(\langle n | \mu_\alpha | j \rangle \langle j | \mu_\beta | n \rangle) \\ &\quad + i\omega \text{Im}(\langle n | \mu_\alpha | j \rangle \langle j | \mu_\beta | n \rangle)] \\ &= G_{\beta\alpha} + iG'_{\beta\alpha}. \end{aligned} \quad (\text{B9})$$

For the last step, we have used $\text{Im}(z^*) = -\text{Im}(z)$, and $\hat{\mu}$ and \hat{m} are Hermitian operators.

To finish defining the complex dynamic molecular property tensors, we incorporate the absorption and dispersion line-shape functions g and f , as described in Appendix C. This is necessary to account for resonant absorption.

Combining everything,

$$\tilde{\alpha}_{\alpha\beta} \simeq [\alpha_{\alpha\beta}(f) + i\alpha_{\alpha\beta}(g)] - i[\alpha'_{\alpha\beta}(f) + i\alpha'_{\alpha\beta}(g)], \quad (\text{B10})$$

where

$$\alpha_{\alpha\beta}(X) = \frac{2}{\hbar} \sum_{j \neq n} (X_{jn}) \omega_{jn} \text{Re}(\langle n | \mu_\alpha | j \rangle \langle j | \mu_\beta | n \rangle), \quad (\text{B11a})$$

$$\alpha'_{\alpha\beta}(X) = -\frac{2}{\hbar} \sum_{j \neq n} (X_{jn}) \omega \text{Im}(\langle n | \mu_\alpha | j \rangle \langle j | \mu_\beta | n \rangle), \quad (\text{B11b})$$

and similarly for the other molecular tensors, where X is replaced with g or f . Inside the sums, X is replaced with X_{jn} (e.g., $f \rightarrow f_{jn}$) to indicate that the line-shape functions depend on the transitions.

For clarity, we also explicitly write the formulas for $\tilde{G}_{\alpha\beta}$ and $\tilde{\mathcal{G}}_{\alpha\beta}$:

$$\tilde{G}_{\alpha\beta} \simeq [G_{\alpha\beta}(f) + iG_{\alpha\beta}(g)] - i[G'_{\alpha\beta}(f) + iG'_{\alpha\beta}(g)], \quad (\text{B12})$$

$$\tilde{\mathcal{G}}_{\alpha\beta} \simeq [G_{\beta\alpha}(f) + iG_{\beta\alpha}(g)] + i[G'_{\beta\alpha}(f) + iG'_{\beta\alpha}(g)], \quad (\text{B13})$$

with

$$G_{\alpha\beta}(X) = \frac{2}{\hbar} \sum_{j \neq n} (X_{jn}) \omega_{jn} \text{Re}(\langle n | \mu_\alpha | j \rangle \langle j | \mu_\beta | n \rangle), \quad (\text{B14a})$$

$$G'_{\alpha\beta}(X) = -\frac{2}{\hbar} \sum_{j \neq n} (X_{jn}) \omega \text{Im}(\langle n | \mu_\alpha | j \rangle \langle j | \mu_\beta | n \rangle), \quad (\text{B14b})$$

$$G_{\beta\alpha}(X) = \frac{2}{\hbar} \sum_{j \neq n} (X_{jn}) \omega_{jn} \text{Re}(\langle n | m_\alpha | j \rangle \langle j | \mu_\beta | n \rangle), \quad (\text{B14c})$$

$$G'_{\beta\alpha}(X) = \frac{2}{\hbar} \sum_{j \neq n} (X_{jn}) \omega \text{Im}(\langle n | m_\alpha | j \rangle \langle j | \mu_\beta | n \rangle). \quad (\text{B14d})$$

We now use the results of the isotropic rotational averaging completed in Appendix E. From Eqs. (E10), (E19), (E30), and (E31), and noting that the quadrupole moments average to zero, for real wave functions we have

$$\tilde{\mu}_\alpha \rightarrow \tilde{\alpha}(\tilde{E}_\alpha)_0 + \tilde{G}(\tilde{B}_\alpha)_0 + \dots, \quad (\text{B15})$$

$$\tilde{m}'_\alpha \rightarrow \tilde{\chi}(\tilde{B}_\alpha)_0 - \tilde{G}(\tilde{E}_\alpha)_0 + \dots. \quad (\text{B16})$$

Correcting for notational differences, $\mu \rightarrow p$, $m' \rightarrow m$, $(\tilde{B}_\alpha)_0 \rightarrow \tilde{B}_\alpha$, and similarly for \tilde{E}_α , we finally have

$$\tilde{\mathbf{p}} \simeq \tilde{\alpha} \tilde{\mathbf{E}} + \tilde{G} \tilde{\mathbf{B}}, \quad \tilde{\mathbf{m}} \simeq \tilde{\chi} \tilde{\mathbf{B}} - \tilde{G} \tilde{\mathbf{E}}.$$

where $\tilde{\alpha}$, $\tilde{\chi}$, and \tilde{G} are scalars defined in Eqs. (E7), (E16), and (E26), respectively.

APPENDIX C: LINE-SHAPE FUNCTIONS g AND f

We follow the formalism in Ref. [1] for this section. The absorption and dispersion line-shape functions g and f , respectively, are necessary to account for absorbing frequencies of a radiation field.

Absorption can be accounted for by changing the frequency (or energy) to be complex:

$$\omega_{jn} \rightarrow \tilde{\omega}_{jn} = \omega_{jn} - \frac{1}{2}i\Gamma_j, \quad (\text{C1})$$

where Γ is the *damping factor* and $1/\Gamma$ is the *lifetime* of the excited state j . For example, for $e^{-i\omega t}$ HTD, including an imaginary frequency effectively introduces damping:

$$e^{-i\omega t} \rightarrow e^{-i(\omega - \frac{1}{2}i\Gamma)t} = e^{-i\omega t} e^{-\frac{1}{2}\Gamma t}. \quad (\text{C2})$$

Since we are interested in the line-shape functions near resonance, as the effect of absorption is small otherwise, we only need to look at the difference term $(\omega_{jn}^2 - \omega^2)$, where $\omega_{jn} \rightarrow \tilde{\omega}_{jn}$:

$$\begin{aligned} \frac{1}{\omega_{jn}^2 - \omega^2} &\rightarrow \frac{1}{(\tilde{\omega}_{jn} - \omega)(\tilde{\omega}_{jn}^* + \omega)} \\ &\simeq \frac{(\omega_{jn}^2 - \omega^2) + i\omega\Gamma_j}{(\omega_{jn}^2 - \omega^2)^2 + \omega^2\Gamma_j^2} \equiv f + ig. \end{aligned} \quad (\text{C3})$$

The line-shape functions g and f are real valued:

$$f = \frac{(\omega_{jn}^2 - \omega^2)}{(\omega_{jn}^2 - \omega^2)^2 + \omega^2\Gamma_j^2}, \quad (\text{C4})$$

$$g = \frac{\omega\Gamma_j}{(\omega_{jn}^2 - \omega^2)^2 + \omega^2\Gamma_j^2}. \quad (\text{C5})$$

We can then use the line-shape functions by setting

$$\frac{1}{\omega_{jn}^2 - \omega^2} \rightarrow f + ig \quad (\text{C6})$$

in Eqs. (B7). For example, for a particular transition $j \leftarrow n$,

$$\alpha_{\alpha\beta} \rightarrow \alpha_{\alpha\beta}(f) + i\alpha_{\alpha\beta}(g), \quad (\text{C7})$$

$$\alpha_{\alpha\beta}(X) = \frac{2}{\hbar} X \omega_{jn} \text{Re}(\langle n | \mu_\alpha | j \rangle \langle j | \mu_\beta | n \rangle), \quad (\text{C8})$$

and similarly for the other molecular tensors, where X is replaced with g or f .

Note that f and g should really be f_{jn} and g_{jn} , since they are dependent on the index and states j and n . Also, f and g may be replaced with the actual line-shape functions of the molecules. It is worth noting that because only g represents the damping factor Γ , dynamic molecular property tensors that are functions of g are responsible for the absorption of radiation. For the molecular tensor $\tilde{\mathcal{G}}_{\alpha\beta}$, we can write

$$\begin{aligned} \tilde{\mathcal{G}}_{\alpha\beta} &\rightarrow \frac{2}{\hbar} \sum_{j \neq n} (f_{jn} + ig_{jn}) [\omega_{jn} \text{Re}(\langle n | m_\alpha | j \rangle \langle j | \mu_\beta | n \rangle) \\ &\quad + i\omega \text{Im}(\langle n | m_\alpha | j \rangle \langle j | \mu_\beta | n \rangle)]. \end{aligned} \quad (\text{C9})$$

APPENDIX D: RANDOM ORIENTATIONAL AVERAGING (ROTATIONAL AVERAGING) OF ISOTROPIC SAMPLES

For isotropic samples, since the orientations of each molecule is randomly distributed about 4π sr, compared to a fixed laboratory frame, we must average over all molecular orientations. The EM fields can be considered fixed, for a given instant in time, in the fixed laboratory frame. The orientational averaging then is a process to average over all possible molecular frame orientations with respect to this laboratory frame. Each molecule has its own molecular frame wherein the molecular property tensors and multipole moments are specified, and each molecular frame coordinate axes are randomly oriented with respect to each other and the fixed laboratory frame. Thus, we can assume a uniformly distributed Euler angle relation between molecular and laboratory frame coordinate axes.

1. Formalism

Craig and Thirunamachandran have nicely summarized orientational averaging using tensors in Ref. [19]. We use their explanation and results, particularly for tensors of rank 2.

Let the components of an n th-rank tensor T with respect to a space-fixed frame be T_{i_1, \dots, i_n} . If T refers to a molecular property, we can express it in terms of a molecule-fixed frame through

$$T_{i_1, \dots, i_n} = l_{i_1 \lambda_1} \dots l_{i_n \lambda_n} T_{\lambda_1, \dots, \lambda_n}, \quad (\text{D1})$$

where $l_{i_p \lambda_p}$ is the cosine of the angle between the space-fixed axis i_p and the molecule-fixed axis λ_p .

Let

$$I^{(n)} \equiv \langle l_{i_1 \lambda_1}, \dots, l_{i_n \lambda_n} \rangle_{\Omega} \quad (\text{D2})$$

be the rotational average ($\langle \dots \rangle_{\Omega}$) of the direction cosine product. Generally, we may then write the rotational average (isotropic orientational average) of a rank n tensor T as [19,20]

$$\langle T_{i_1, \dots, i_n} \rangle_{\Omega} = \langle l_{i_1 \lambda_1}, \dots, l_{i_n \lambda_n} T_{\lambda_1 \lambda_2, \dots, \lambda_n} \rangle_{\Omega} = I^{(n)} T_{\lambda_1 \lambda_2, \dots, \lambda_n}. \quad (\text{D3})$$

For rank 2 tensors, we have

$$I^{(2)} = \frac{1}{3} \delta_{i_1 i_2} \delta_{\lambda_1 \lambda_2}, \quad (\text{D4})$$

where δ_{ij} is the Kronecker δ .

2. Example

Let us apply this rotational averaging using a relevant example. We want to show

$$\langle (\mathbf{E} \cdot \mathbf{p})(\mathbf{B} \cdot \mathbf{m}) \rangle_{\Omega} = \frac{1}{3} \langle (\mathbf{E} \cdot \mathbf{B})(\mathbf{p} \cdot \mathbf{m}) \rangle_{\Omega}. \quad (\text{D5})$$

We may assume \mathbf{E} and \mathbf{B} are external fields that are fixed relative to the fixed laboratory frame, for all molecules. So we can take them out and rotationally average over the tensor that actually varies over the random molecular distribution. We also assume the molecules are identical to each other, once their molecular coordinates are matched, since the sample is isotropic.

We use Einstein notation here where like indices imply a sum over that index. Let $T_{lm} = p_l m_m$. Then,

$$\begin{aligned} \langle (\mathbf{E} \cdot \mathbf{p})(\mathbf{B} \cdot \mathbf{m}) \rangle_{\Omega} &= (E_i \delta_{il})(B_j \delta_{jm}) \langle p_l m_m \rangle_{\Omega} \\ &= (E_i \delta_{il})(B_j \delta_{jm}) I_{lm, \lambda \mu}^{(2)} (T_{\lambda \mu}) \\ &= \frac{1}{3} \langle (\mathbf{E} \cdot \mathbf{B})(\mathbf{p} \cdot \mathbf{m}) \rangle_{\Omega}. \end{aligned} \quad (\text{D6})$$

From this simple derivation, we can see that $\langle (\mathbf{E} \cdot \mathbf{p})(\mathbf{B} \cdot \mathbf{m}) \rangle_{\Omega} = 0$ if $(\mathbf{E} \cdot \mathbf{B}) = 0$ or $(\mathbf{p} \cdot \mathbf{m}) = 0$. This seems to be because $(\mathbf{E} \cdot \mathbf{p}) = Ep \cos(\theta_{Ep})$ and $(\mathbf{B} \cdot \mathbf{m}) = Bm \cos(\theta_{Bm})$ become like ‘‘linearly independent angles’’ to each other, so it is akin to $\langle (\mathbf{E} \cdot \mathbf{p})(\mathbf{B} \cdot \mathbf{m}) \rangle_{\Omega} \sim \langle \cos \theta_{Ep} \rangle_{\Omega} \langle \cos \theta_{Bm} \rangle_{\Omega} = 0 * 0 = 0$. This shows that only the components that have $(\mathbf{E} \cdot \mathbf{B} \neq 0)$ or $(\mathbf{p} \cdot \mathbf{m} \neq 0)$ contribute to the rotational average in a nonzero way, that is, only the \mathbf{B} component parallel to \mathbf{E} and same for \mathbf{p} and \mathbf{m} contribute to $\langle (\mathbf{E} \cdot \mathbf{p})(\mathbf{B} \cdot \mathbf{m}) \rangle_{\Omega}$.

APPENDIX E: ORIENTATIONAL AVERAGING OF MOLECULAR PROPERTY TENSORS FOR ISOTROPIC SAMPLES

In this section, we apply isotropic rotational averaging to the complex dynamic molecular property tensors, which are the complex quantities of those found in Eqs. (B7). We assume each transition (resonance) can be averaged independently of each other. Also note that rotational averaging is a linear operation with real weighting factors, so that

$$\langle \text{Re}(T) \rangle_{\Omega} = \text{Re}(\langle T \rangle_{\Omega}), \quad (\text{E1a})$$

$$\langle \text{Im}(T) \rangle_{\Omega} = \text{Im}(\langle T \rangle_{\Omega}). \quad (\text{E1b})$$

1. Electric-quadrupole moment, $\langle \Theta_{\beta\gamma} \rangle_{\Omega}$

The electric-quadrupole moment averages to zero for isotropic samples and is not included as one of the multipole moments, even though it has the same magnitude as the magnetic dipole [19,20]. For the same reason, the molecular property tensors $A_{\alpha, \beta\gamma}, A'_{\alpha, \beta\gamma}, D_{\alpha, \beta\gamma}$, and $D'_{\alpha, \beta\gamma}$ also average out to zero. Then we have

$$\langle \tilde{A}_{\alpha, \beta\gamma} \rangle_{\Omega} = 0, \quad (\text{E2})$$

$$\langle \tilde{D}_{\alpha, \beta\gamma} \rangle_{\Omega} = 0. \quad (\text{E3})$$

2. Electric polarizability tensor, $\langle \tilde{\alpha}_{\alpha\beta} \rangle_{\Omega}$

For the complex electric polarizability tensor, $\tilde{\alpha}_{\alpha\beta}$ we are interested in the rotational average of

$$T_{\alpha\beta}^{(\alpha)} = (\langle n | \mu_{\alpha} | j \rangle \langle j | \mu_{\beta} | n \rangle). \quad (\text{E4})$$

Using Eqs. (D3) and (D4),

$$\begin{aligned} \langle T_{\alpha\beta}^{(\alpha)} \rangle_{\Omega} &= \frac{1}{3} \delta_{\alpha\beta} \langle T_{\lambda\lambda}^{(\alpha)} \rangle_{\Omega} = \frac{1}{3} \delta_{\alpha\beta} \langle \langle n | \mu_{\lambda} | j \rangle \langle j | \mu_{\lambda} | n \rangle \rangle_{\Omega} \\ &= \frac{1}{3} \delta_{\alpha\beta} \langle \langle n | \mu_{\lambda} | j \rangle \langle n | \mu_{\lambda}^{\dagger} | j \rangle^* \rangle_{\Omega} \\ &= \frac{1}{3} \delta_{\alpha\beta} \langle \langle n | \mu_{\lambda} | j \rangle \langle n | \mu_{\lambda} | j \rangle^* \rangle_{\Omega} \\ &= \frac{1}{3} \delta_{\alpha\beta} \sum_{\lambda} |\langle n | \mu_{\lambda} | j \rangle|^2 \in \mathbb{R}. \end{aligned} \quad (\text{E5})$$

From this and Eq. (B11b), we see that

$$\langle \alpha'_{\alpha\beta}(X) \rangle_{\Omega} \rightarrow 0. \quad (\text{E6})$$

Then from Eqs. (B10) and (B11b), we obtain the isotropic average of the complex electric polarizability:

$$\langle \tilde{\alpha}_{\alpha\beta} \rangle_{\Omega} \simeq \delta_{\alpha\beta} \langle \tilde{\alpha} \rangle \equiv \delta_{\alpha\beta} (\alpha' + i\alpha''), \quad (\text{E7})$$

where

$$\alpha' = \frac{2}{\hbar} \sum_{j \neq n} (f_{jn}) \omega_{jn} \left(\frac{1}{3} \sum_{\lambda} |\langle n | \mu_{\lambda} | j \rangle|^2 \right) \in \mathbb{R}, \quad (\text{E8})$$

$$\alpha'' = \frac{2}{\hbar} \sum_{j \neq n} (g_{jn}) \omega_{jn} \left(\frac{1}{3} \sum_{\lambda} |\langle n | \mu_{\lambda} | j \rangle|^2 \right) \in \mathbb{R}. \quad (\text{E9})$$

Thus, we have explicitly shown that the complex electric polarizability tensor, when isotropically averaged, becomes a complex scalar, and can be rewritten in Eq. (B3) as

$$\tilde{\alpha}_{\alpha\beta}(\tilde{E}_{\beta})_0 \rightarrow \tilde{\alpha}(\tilde{E}_{\alpha})_0. \quad (\text{E10})$$

3. Magnetic susceptibility tensor, $\langle \tilde{\chi}_{\alpha\beta} \rangle_{\Omega}$

For the complex magnetic susceptibility tensor, $\tilde{\chi}_{\alpha\beta}$ we follow a very similar method to that for $\tilde{\alpha}_{\alpha\beta}$. We are interested in the rotational average of

$$T_{\alpha\beta}^{(X)} = (\langle n | m_{\alpha} | j \rangle \langle j | m_{\beta} | n \rangle), \quad (\text{E11})$$

and

$$T_{\alpha\beta}^{(X)} = \sum_i \frac{e_i^2}{4m_i} \langle n | r_{i\alpha} r_{i\beta} - r_i^2 \delta_{\alpha\beta} | n \rangle. \quad (\text{E12})$$

Then,

$$\langle T_{\alpha\beta}^{(\chi)} \rangle_{\Omega} = \frac{1}{3} \delta_{\alpha\beta} \sum_{\lambda} |\langle n | m_{\lambda} | j \rangle|^2 \in \mathbb{R}, \quad (\text{E13})$$

$$\langle T_{\alpha\beta}^{(\chi')} \rangle_{\Omega} = -\frac{2}{3} \delta_{\alpha\beta} \sum_i \left[\frac{e_i^2}{4m_i} \langle n | r_i^2 | n \rangle \right] \in \mathbb{R}. \quad (\text{E14})$$

From this, we see that

$$\langle \chi'_{\alpha\beta}(X) \rangle_{\Omega} \rightarrow 0. \quad (\text{E15})$$

We obtain the isotropic average of the complex magnetic susceptibility:

$$\langle \tilde{\chi}_{\alpha\beta} \rangle_{\Omega} \simeq \delta_{\alpha\beta} \langle \tilde{\chi} \rangle \equiv \delta_{\alpha\beta} (\chi' + i\chi''), \quad (\text{E16})$$

with

$$\begin{aligned} \chi' &= \frac{2}{\hbar} \sum_{j \neq n} (f_{jn}) \omega_{jn} \left(\frac{1}{3} \sum_{\lambda} |\langle n | m_{\lambda} | j \rangle|^2 \right) \\ &+ \left(-\frac{2}{3} \sum_i \left[\frac{e_i^2}{4m_i} \langle n | r_i^2 | n \rangle \right] \right) \in \mathbb{R}, \quad (\text{E17}) \end{aligned}$$

$$\chi'' = \frac{2}{\hbar} \sum_{j \neq n} (g_{jn}) \omega_{jn} \left(\frac{1}{3} \sum_{\lambda} |\langle n | m_{\lambda} | j \rangle|^2 \right) \in \mathbb{R}. \quad (\text{E18})$$

We have shown that the complex magnetic susceptibility tensor, when isotropically averaged, becomes a complex scalar and can be rewritten in Eq. (B4) as

$$\tilde{\chi}_{\alpha\beta}(\tilde{B}_{\beta})_0 \rightarrow \tilde{\chi}(\tilde{B}_{\alpha})_0. \quad (\text{E19})$$

4. Mixed electric-magnetic dipole polarizability tensors,

$$\langle \tilde{G}_{\alpha\beta} \rangle_{\Omega} \text{ and } \langle \tilde{\mathcal{G}}_{\alpha\beta} \rangle_{\Omega}$$

For the complex mixed electric-magnetic dipole polarizability tensors, $\tilde{G}_{\alpha\beta}$ and $\tilde{\mathcal{G}}_{\alpha\beta}$, we are interested in the rotational average of

$$T_{\alpha\beta}^{(G)} = (\langle n | \mu_{\alpha} | j \rangle \langle j | m_{\beta} | n \rangle), \quad (\text{E20})$$

$$T_{\alpha\beta}^{(G')} = (\langle n | m_{\alpha} | j \rangle \langle j | \mu_{\beta} | n \rangle). \quad (\text{E21})$$

Then,

$$\langle T_{\alpha\beta}^{(G)} \rangle_{\Omega} = \frac{1}{3} \delta_{\alpha\beta} \sum_{\lambda} (\langle n | \mu_{\lambda} | j \rangle \langle j | m_{\lambda} | n \rangle) \in \mathbb{C}, \quad (\text{E22})$$

$$\langle T_{\alpha\beta}^{(G')} \rangle_{\Omega} = \frac{1}{3} \delta_{\alpha\beta} \sum_{\lambda} (\langle n | m_{\lambda} | j \rangle \langle j | \mu_{\lambda} | n \rangle) \in \mathbb{C}. \quad (\text{E23})$$

Here we use real wave functions to calculate the multipole moments for $\tilde{G}_{\alpha\beta}$ and $\tilde{\mathcal{G}}_{\alpha\beta}$. For real wave functions, $\langle j | \hat{\mu} | n \rangle$ and $\langle j | \hat{m} | n \rangle$ are purely real and purely imaginary, respectively, for $j \neq n$ [19]. Then

$$\langle T_{\alpha\beta}^{(G)} \rangle_{\Omega} \text{ and } \langle T_{\alpha\beta}^{(G')} \rangle_{\Omega} \in \text{Purely Imaginary.}$$

We then have

$$\langle G_{\alpha\beta}(X) \rangle_{\Omega} \text{ and } \langle G_{\beta\alpha}(X) \rangle_{\Omega} \rightarrow 0, \quad (\text{E24})$$

and

$$\begin{aligned} \langle T_{\alpha\beta}^{(G)} \rangle_{\Omega} &= i \text{Im} [\langle T_{\alpha\beta}^{(G)} \rangle_{\Omega}] = -i \text{Im} [\langle T_{\alpha\beta}^{(G)} \rangle_{\Omega}^*] \\ &= -i \text{Im} [\langle T_{\alpha\beta}^{(G')} \rangle_{\Omega}] = -\langle T_{\alpha\beta}^{(G')} \rangle_{\Omega}. \quad (\text{E25}) \end{aligned}$$

With these equations, we can then conclude with the final form of the isotropic average of the complex mixed electric-magnetic dipole polarizability tensors:

$$\langle \tilde{G}_{\alpha\beta} \rangle_{\Omega} \simeq \delta_{\alpha\beta} [G'(g) - iG'(f)] \equiv \delta_{\alpha\beta} \tilde{G}, \quad (\text{E26})$$

$$\langle \tilde{\mathcal{G}}_{\alpha\beta} \rangle_{\Omega} \simeq \delta_{\alpha\beta} [-G'(g) + iG'(f)] = -\delta_{\alpha\beta} \tilde{G}, \quad (\text{E27})$$

where

$$\begin{aligned} G'(X) &= -\frac{2}{\hbar} \sum_{j \neq n} (X_{jn}) \omega_{jn} \left(\frac{1}{3} \sum_{\lambda} \text{Im} (\langle n | \mu_{\lambda} | j \rangle \langle j | m_{\lambda} | n \rangle) \right) \in \mathbb{R}. \quad (\text{E28}) \end{aligned}$$

Note that here, the scalar $G'(X)$ denotes the isotropic average of Eqs. (B7f) and (B14b), that is,

$$G'(X) \equiv \langle G'_{\alpha\beta}(X) \rangle_{\Omega}. \quad (\text{E29})$$

We also note that depending on the ordering, or the orientations (with respect to each other), of $\hat{\mu}$ and \hat{m} , the signs of $\langle \tilde{G}_{\alpha\beta} \rangle_{\Omega}$ and $\langle \tilde{\mathcal{G}}_{\alpha\beta} \rangle_{\Omega}$ may change.

We can then rewrite the respective parts in Eqs. (B3) and (B4) as

$$\tilde{G}_{\alpha\beta}(\tilde{B}_{\beta})_0 \rightarrow \tilde{G}(\tilde{B}_{\alpha})_0, \quad (\text{E30})$$

$$\tilde{\mathcal{G}}_{\alpha\beta}(\tilde{E}_{\beta})_0 \rightarrow -\tilde{G}(\tilde{E}_{\alpha})_0. \quad (\text{E31})$$

APPENDIX F: DERIVATION OF GENERALIZED OPTICAL CHIRALITY C_g

We begin with $\omega \text{Im}(\tilde{\mathbf{E}}^* \cdot \tilde{\mathbf{B}})$ from Eq. (16). Note that this is time-independent for monochromatic fields. We first derive the following identity, given in Ref. [3]:

$$\begin{aligned} \tilde{\mathbf{B}} \cdot \mathbf{E} - \tilde{\mathbf{E}} \cdot \mathbf{B} &= -\frac{i\omega}{4} [(\tilde{\mathbf{B}} - \tilde{\mathbf{B}}^*) \cdot (\tilde{\mathbf{E}} + \tilde{\mathbf{E}}^*) - (\tilde{\mathbf{E}} - \tilde{\mathbf{E}}^*) \cdot (\tilde{\mathbf{B}} + \tilde{\mathbf{B}}^*)] \\ &= \omega \text{Im}(\tilde{\mathbf{E}}^* \cdot \tilde{\mathbf{B}}). \quad (\text{F1}) \end{aligned}$$

Now using the Maxwell equations for a linear medium with no free current or charges, we can rewrite the identity (F1):

$$\begin{aligned} \omega \text{Im}(\tilde{\mathbf{E}}^* \cdot \tilde{\mathbf{B}}) &= \tilde{\mathbf{B}} \cdot \mathbf{E} - \tilde{\mathbf{E}} \cdot \mathbf{B} \\ &= -\nabla \times \mathbf{E} \cdot \mathbf{E} - \frac{1}{\epsilon\mu} \mathbf{B} \cdot \nabla \times \mathbf{B} \\ &= -\frac{2}{\epsilon} \left[\frac{\epsilon}{2} \mathbf{E} \cdot (\nabla \times \mathbf{E}) + \frac{1}{2\mu} \mathbf{B} \cdot (\nabla \times \mathbf{B}) \right], \quad (\text{F2}) \end{aligned}$$

where ϵ and μ are the electric permittivity and the magnetic permeability, respectively [21]. In vacuum,

$$\epsilon \rightarrow \epsilon_0, \quad \mu \rightarrow \mu_0.$$

We can now define the *generalized optical chirality* C_g :

$$C_g \equiv \frac{\epsilon}{2} \mathbf{E} \cdot (\nabla \times \mathbf{E}) + \frac{1}{2\mu} \mathbf{B} \cdot (\nabla \times \mathbf{B}). \quad (\text{F3})$$

As would be expected, this simply replaces the vacuum permittivity and permeability in the optical chirality C , in Ref. [3], with those for a linear medium. Bliokh defined a

similar, but slightly different [apart from the (c/ω) factor], chirality density χ [8]. Our C_g is applicable for EM fields in a linear medium, with no free current or charges.

Summarizing,

$$\begin{aligned}\omega \text{Im}(\tilde{\mathbf{E}}^* \cdot \tilde{\mathbf{B}}) &= \mathbf{B} \cdot \mathbf{E} - \dot{\mathbf{E}} \cdot \mathbf{B} \\ &= -\frac{2}{\epsilon} \left[\frac{\epsilon}{2} \mathbf{E} \cdot (\nabla \times \mathbf{E}) + \frac{1}{2\mu} \mathbf{B} \cdot (\nabla \times \mathbf{B}) \right] \\ &\equiv -\frac{2}{\epsilon} C_g.\end{aligned}\quad (\text{F4})$$

As a special case, let us consider the optical chirality of a CPL in a linear medium. From Appendix F, we use Eqs. (H1) and (H2) for C_g :

$$\begin{aligned}C_g^{(L/R)} &= \pm k^{(L/R)} \left[\frac{\epsilon}{2} |\mathbf{E}^{(L/R)}|^2 + \frac{1}{2\mu} |\mathbf{B}^{(L/R)}|^2 \right] \\ &= \pm k^{(L/R)} [U_e^{(L/R)} + U_b^{(L/R)}] = \pm 2k^{(L/R)} U_e^{(L/R)} \\ &= \pm \frac{2\omega U_e^{(L/R)}}{c} n^{(L/R)}.\end{aligned}\quad (\text{F5})$$

The (+) sign is for LCPL (L), and the (−) sign is for RCPL (R); n is the index of refraction. From this we see that for monochromatic CPLs, time invariance of the optical chirality is equivalent to conservation of energy of the fields.

APPENDIX G: ORDER OF MAGNITUDE ESTIMATIONS

Here we develop order of magnitude estimates for the parameters $(n^2\chi)/(c^2\alpha)$, $\Delta n/n$, and g_{CPL} . This will be helpful for knowing if and when these terms can be dropped, as well as estimating physically valid regions for the dissymmetry factor g .

From Ref. [19], for a one-photon absorption process, the matrix transition element for the electric dipole is given by

$$M_{fi}(\xi) = -i \left(\frac{n\hbar ck}{2\epsilon_0 V} \right)^{1/2} \mathbf{e}^{(\lambda)}(\mathbf{k}) \cdot \boldsymbol{\mu}^{m0}(\xi) e^{i\mathbf{k}\cdot\mathbf{R}_\xi}, \quad (\text{G1})$$

where $\boldsymbol{\mu}$ is the electric dipole, and the total transition rate from the Fermi golden rule is given by

$$\Gamma = \frac{2\pi}{\hbar} \rho \sum_{\xi} |M_{fi}(\xi)|^2. \quad (\text{G2})$$

For magnetic dipole transitions,

$$M_{fi} = -i \left(\frac{n\hbar k}{2\epsilon_0 c V} \right)^{1/2} b_i^{(\lambda)}(\mathbf{k}) m_i^{m0} e^{i\mathbf{k}\cdot\mathbf{R}}, \quad (\text{G3})$$

where (m) is the magnetic dipole.

The authors then state that the matrix element from Eq. (G3) is typically smaller than its electric analog in Eq. (G1) by about 10^{-3} – 10^{-2} . In Eqs. (G1) and (G3), b has the same unit as e , and the magnetic field $B \sim b/c \sim e/c$, where the electric field $E \sim e$. From this, we can see that

$$\begin{aligned}\frac{1}{c} |\mathbf{b} \cdot \mathbf{m}|^2 &\simeq (10^{-3}\text{--}10^{-2})^2 c |\mathbf{e} \cdot \boldsymbol{\mu}|^2 \\ &\Rightarrow \frac{m}{c} \simeq (10^{-3}\text{--}10^{-2}) \mu.\end{aligned}\quad (\text{G4})$$

With this relationship, we can then derive order of magnitude estimates for the molecular property tensors given

in Eqs. (B7):

$$\begin{aligned}\left(\frac{\chi}{c^2} \right) &\sim \left(\frac{m}{c} \right)^2 \simeq (10^{-3}\text{--}10^{-2})^2 \mu^2 \sim (10^{-6}\text{--}10^{-4}) \alpha \\ &\Rightarrow \gamma = \frac{\chi n^2}{\alpha c^2} \simeq (10^{-6}\text{--}10^{-4}),\end{aligned}\quad (\text{G5a})$$

$$\begin{aligned}g_{\text{CPL}} &= -4 \frac{G'(g)n}{\alpha'' c} \sim \frac{1}{c} \frac{\boldsymbol{\mu} \cdot \mathbf{m}}{\boldsymbol{\mu} \cdot \boldsymbol{\mu}} \sim \frac{m}{\mu c} \\ &\Rightarrow g_{\text{CPL}} \simeq (10^{-3}\text{--}10^{-2}),\end{aligned}\quad (\text{G5b})$$

$$\begin{aligned}\frac{\Delta n}{n_{\text{ave}}^0} &= \frac{n^L - n^R}{n^L + n^R} = \frac{1}{2} \frac{n^L - n^R}{\frac{1}{2}(n^L + n^R)} = \frac{1}{2} g_{\text{ORD}} \\ &\Rightarrow \frac{\Delta n}{n_{\text{ave}}^0} \simeq (10^{-3}\text{--}10^{-2}).\end{aligned}\quad (\text{G5c})$$

g_{ORD} is the dissymmetry factor for optical rotation, as opposed to the dissymmetry factor for absorption [e.g., Eq. (G5b)]. g_{CD} and g_{ORD} are related by Kramers-Kronig relations (see Appendix I). For the last step, we used the fact that they are approximately the same order of magnitude. We can see why γ , or terms with χ when compared with α , tend to be dropped, and for good reason.

APPENDIX H: CIRCULAR POLARIZATION AND COUNTERPROPAGATING LCPL + RCPL FORMALISM (SWCF)

Let us first review the definition of LCPL and RCPL. Right-circularly polarized light (RCPL) rotates clockwise (CW) over time when viewed towards the source, for a fixed spatial plane ($z = 0$, for example, for light propagating in the z direction) [1]. Or, for fixed time, we can wrap our right hands around the turning electric field vector, with thumbs and fingertips pointing in the direction of propagation. Left-circularly polarized light (LCPL) rotates counterclockwise (CCW) over time, when viewed towards the source, for a fixed spatial plane. Or, for fixed time, we can wrap our left hands around the propagating electric field.

For the theory of the SWCF standing waves created by counterpropagating CPLs, we assumed normally incident reflection and ignored boundary conditions for the chiral material. We also assumed that all the EM waves have the same monochromatic angular frequency ω .

1. Useful CPL identities

Here we develop some useful properties of monochromatic CPL fields that will be helpful. These can be verified from the explicit formulas of CPL fields traveling in both $\pm\mathbf{z}$ directions, as given in Eqs. (H5) and (H16).

Since we are interested in the optical chirality, we first state the following relations for the curl of the EM fields:

$$\nabla \times \mathbf{E}^L = +k^L \mathbf{E}^L, \quad (\text{H1a})$$

$$\nabla \times \mathbf{E}^R = -k^R \mathbf{E}^R, \quad (\text{H1b})$$

$$\nabla \times \mathbf{B}^L = +k^L \mathbf{B}^L, \quad (\text{H1c})$$

$$\nabla \times \mathbf{B}^R = -k^R \mathbf{B}^R, \quad (\text{H1d})$$

where $k = |\mathbf{k}| = n\omega/c$ is the wave vector magnitude, L is for LCPL, and R is for RCPL. These equations are general, and

are independent of coordinates because the handedness of CPL is defined in terms of the propagation vector \mathbf{k} .

Let us also calculate the total energy density for CPL:

$$\begin{aligned} U_{\text{tot}} &= U_e + U_b = \frac{\epsilon}{2} |\mathbf{E}|^2 + \frac{1}{2\mu} |\mathbf{B}|^2 \\ &= \left(\frac{\epsilon}{2} + \frac{n^2}{2\mu c^2} \right) |\mathbf{E}|^2 = 2 \left(\frac{\epsilon}{2} \right) |\mathbf{E}|^2 = 2U_e. \end{aligned} \quad (\text{H2a})$$

$$\therefore U_{\text{tot}}^{(L/R)} = 2U_e^{(L/R)} = 2 \left(\frac{\epsilon^{(L/R)}}{2} \right) |\mathbf{E}^{(L/R)}|^2. \quad (\text{H2b})$$

Here, $|\mathbf{E}|^2 = \mathbf{E} \cdot \mathbf{E}$ and $|\mathbf{B}|^2 = \mathbf{B} \cdot \mathbf{B}$, and both are constant over time, so U_e and U_b are also time invariant.

Recall that the real physical EM fields are obtained by taking the real parts of the complex EM fields, as shown in Eq. (7), that is,

$$\mathbf{E} = \text{Re}\{\tilde{\mathbf{E}}\} = \frac{1}{2}[\tilde{\mathbf{E}} + \tilde{\mathbf{E}}^*], \text{ etc.}$$

We maintain that here, and for such, we can see that for the EM CPL waves defined as in Eqs. (H5) and (H16), we have the following identities:

$$\tilde{\mathbf{E}}_i \cdot \tilde{\mathbf{E}}_i = 0, \quad \tilde{\mathbf{B}}_i \cdot \tilde{\mathbf{B}}_i = 0, \quad (\text{H3a})$$

$$\begin{aligned} |\mathbf{E}_i|^2 &= \mathbf{E}_i \cdot \mathbf{E}_i = \frac{1}{4}(\tilde{\mathbf{E}}_i + \tilde{\mathbf{E}}_i^*) \cdot (\tilde{\mathbf{E}}_i + \tilde{\mathbf{E}}_i^*) \\ &= \frac{1}{4}(\tilde{\mathbf{E}}_i \cdot \tilde{\mathbf{E}}_i + \tilde{\mathbf{E}}_i \cdot \tilde{\mathbf{E}}_i^* + \text{c.c.}) \\ &= \frac{1}{2}(\tilde{\mathbf{E}}_i \cdot \tilde{\mathbf{E}}_i^*) = \frac{1}{2}|\tilde{\mathbf{E}}_i|^2 = (E_i)^2, \end{aligned} \quad (\text{H3b})$$

$$|\mathbf{B}_i|^2 = \mathbf{B}_i \cdot \mathbf{B}_i = \frac{1}{2}|\tilde{\mathbf{B}}_i|^2 = \frac{1}{2} \left| \frac{n_i}{c} \tilde{\mathbf{E}}_i \right|^2 = \left(\frac{n_i}{c} E_i \right)^2, \quad (\text{H3c})$$

$$\begin{aligned} \mathbf{E}_1 \cdot \mathbf{E}_2 &= \frac{1}{4}(\tilde{\mathbf{E}}_1 \cdot \tilde{\mathbf{E}}_2^* + \text{c.c.}) = \frac{1}{2} \text{Re}(\tilde{\mathbf{E}}_1 \cdot \tilde{\mathbf{E}}_2^*) \\ &= -E_1 E_2 \cos[z(k_1 + k_2)], \end{aligned} \quad (\text{H3d})$$

$$\begin{aligned} \mathbf{B}_1 \cdot \mathbf{B}_2 &= \frac{1}{4}(\tilde{\mathbf{B}}_1 \cdot \tilde{\mathbf{B}}_2^* + \text{c.c.}) = \frac{1}{2} \text{Re}(\tilde{\mathbf{B}}_1 \cdot \tilde{\mathbf{B}}_2^*) \\ &= -\frac{1}{2} \frac{n_1 n_2}{c^2} \text{Re}(\tilde{\mathbf{E}}_1 \cdot \tilde{\mathbf{E}}_2^*) \\ &= \frac{n_1 n_2}{c^2} E_1 E_2 \cos[z(k_1 + k_2)], \end{aligned} \quad (\text{H3e})$$

where $i = 1, 2$; c.c. = complex conjugate. For the (−) configuration, Eqs. (H3) also hold, with the EM fields being replaced with their respective prime (′) fields. From here, it is clear that E_1 and E_2 in Eqs. (H5) and (H16) are indeed the amplitudes of the electric fields.

2. “Left” (+) counterpropagating CPLs

We begin with what we define the left-handed (+) SWCF arrangement to be that given in Fig. 8, where the incident field is LCPL. If left-handed (+) is defined as the incident field being RCPL instead, then the results would differ by a sign change only.

Let \mathbf{E}_1 be an LCPL traveling in the $-z$ direction and \mathbf{E}_2 be the RCPL traveling in the $+z$ direction after the reflection. The boundary conditions to match, for normal incidence of the real EM fields, are

$$\text{At } (z = 0): \quad \mathbf{E}_1 = -\mathbf{E}_2, \quad \mathbf{B}_1 = \mathbf{B}_2. \quad (\text{H4})$$

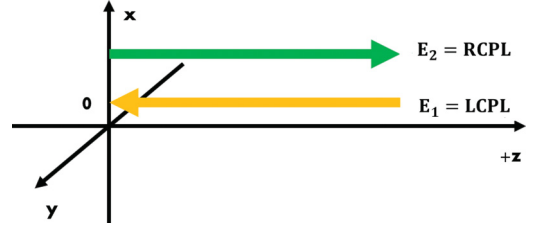


FIG. 8. (Color online) Left-handed (+) SWCF arrangement. Incident electric field is LCPL (with amplitude E_1), traveling from right to left, consistent with Ref. [3]. $E_1 > E_2$ because reflectivity $R < 1$. Reflection occurs at $z = 0$.

The complex EM waves for this (+) standing wave can then be written as

$$\tilde{\mathbf{E}}_1 = E_1(-\hat{\mathbf{x}} + i\hat{\mathbf{y}})e^{i(-k_1 z - \omega t)} \quad (\text{LCPL}), \quad (\text{H5a})$$

$$\tilde{\mathbf{E}}_2 = E_2(+\hat{\mathbf{x}} - i\hat{\mathbf{y}})e^{i(+k_2 z - \omega t)} \quad (\text{RCPL}), \quad (\text{H5b})$$

$$\tilde{\mathbf{B}}_1 = -i \frac{n_1}{c} \tilde{\mathbf{E}}_1, \quad (\text{H5c})$$

$$\tilde{\mathbf{B}}_2 = +i \frac{n_2}{c} \tilde{\mathbf{E}}_2, \quad (\text{H5d})$$

where $(E_1, E_2 \in \mathbb{R})$ are the amplitudes of the electric fields. Also,

$$\begin{aligned} k_1 &= k^L = \frac{n^L \omega}{c}, \quad k_2 = k^R = \frac{n^R \omega}{c}, \\ n_1 &= n^L, \quad n_2 = n^R. \end{aligned} \quad (\text{H6})$$

a. Calculating C_g^+

We wish to obtain the optical chirality C_g^+ for this configuration of EM fields. Recall from Eq. (19),

$$\begin{aligned} C_g^+ &\equiv \left[\frac{\epsilon}{2} \mathbf{E} \cdot (\nabla \times \mathbf{E}) + \frac{1}{2\mu} \mathbf{B} \cdot (\nabla \times \mathbf{B}) \right]^+ \\ &= \left[\frac{\epsilon^+}{2} \mathbf{E}^+ \cdot (\nabla \times \mathbf{E})^+ + \frac{1}{2\mu^+} \mathbf{B}^+ \cdot (\nabla \times \mathbf{B})^+ \right]. \end{aligned} \quad (\text{H7})$$

Since both LCPL and RCPL are present, both n^L and n^R indices of refraction need to be considered appropriately, in determining C_g^+ . To simplify this complication, we use the original identity from Eq. (F4):

$$-\frac{2}{\epsilon^\pm} C_g^\pm = \omega \text{Im}(\tilde{\mathbf{E}}^* \cdot \tilde{\mathbf{B}})^\pm. \quad (\text{H8})$$

We now calculate C_g^+ :

$$\begin{aligned} \text{Im}(\tilde{\mathbf{E}}^* \cdot \tilde{\mathbf{B}})^+ &= \text{Im}[(\tilde{\mathbf{E}}_1 + \tilde{\mathbf{E}}_2)^* \cdot (\tilde{\mathbf{B}}_1 + \tilde{\mathbf{B}}_2)] \\ &= \frac{1}{c} \text{Im}[-in_1 |\tilde{\mathbf{E}}_1|^2 + in_2 |\tilde{\mathbf{E}}_2|^2 \\ &\quad - in_1 \tilde{\mathbf{E}}_1 \cdot \tilde{\mathbf{E}}_2^* + in_2 \tilde{\mathbf{E}}_1^* \cdot \tilde{\mathbf{E}}_2]. \\ \therefore \frac{2}{\epsilon^+} C_g^+ &= -\frac{2\omega}{c} [-n^L E_1^2 + n^R E_2^2 \\ &\quad + E_1 E_2 (n^L - n^R) \cos(zk_{\text{tot}})], \end{aligned} \quad (\text{H9})$$

where $k_{\text{tot}} = (k^L + k^R)$.

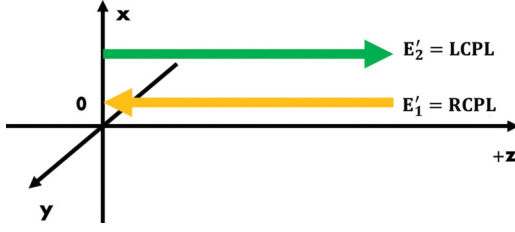


FIG. 9. (Color online) Right-handed (–) SWCF arrangement. Incident electric field is RCPL (with amplitude E'_1), traveling from right to left. $E'_1 > E'_2$ because reflectivity $R < 1$. Reflection occurs at $z = 0$.

b. Calculating U_γ^+

Another quantity of interest is the field energy density term U_γ^\pm from the achiral part of the absorption rate in Eq. (21b). Let us first obtain $\frac{2}{\epsilon^+}U_\gamma^+$ for the (+) configuration. We derive the following terms, using Eqs. (H3):

$$|\tilde{\mathbf{E}}^+|^2 = (\tilde{\mathbf{E}}_1 + \tilde{\mathbf{E}}_2)^* \cdot (\tilde{\mathbf{E}}_1 + \tilde{\mathbf{E}}_2) = 2[E_1^2 + E_2^2 - 2E_1E_2 \cos(k_{\text{tot}}z)], \quad (\text{H10a})$$

$$|\tilde{\mathbf{B}}^+|^2 = |\tilde{\mathbf{B}}_1|^2 + |\tilde{\mathbf{B}}_2|^2 + 2\text{Re}(\tilde{\mathbf{B}}_1 \cdot \tilde{\mathbf{B}}_2^*) = \frac{2}{c^2}[(n_1E_1)^2 + (n_2E_2)^2 + 2n_1n_2E_1E_2 \cos(k_{\text{tot}}z)], \quad (\text{H10b})$$

where

$$k_{\text{tot}} \equiv (k^L + k^R) = 2k_{\text{ave}}, \quad (\text{H11})$$

$$k_{\text{ave}} \equiv \frac{k^L + k^R}{2} = \frac{\omega}{c}n_{\text{ave}}^0. \quad (\text{H12})$$

Then, from Eq. (23),

$$\begin{aligned} \frac{2}{\epsilon^+}U_\gamma^+ &= \frac{1}{2} \left(|\tilde{\mathbf{E}}^+|^2 + \frac{\chi''}{\alpha''} |\tilde{\mathbf{B}}^+|^2 \right) \\ &= E_1^2(1 + \gamma^L) + E_2^2(1 + \gamma^R) \\ &\quad + 2E_1E_2(\sqrt{\gamma^L\gamma^R} - 1) \cos(k_{\text{tot}}z), \end{aligned} \quad (\text{H13})$$

where, from Eq. (21d),

$$\gamma^L \equiv \frac{(n^L)^2\chi''}{c^2\alpha''}, \quad \gamma^R \equiv \frac{(n^R)^2\chi''}{c^2\alpha''}. \quad (\text{H14})$$

3. “Right” (–) counterpropagating CPLs

We proceed to what we define as the right-handed (–) SWCF arrangement, as given in Fig. 9, where the incident field is RCPL now. The equations are almost identical to that for the left (+) arrangement, with (+) \rightarrow (–) and $\mathbf{E}, \mathbf{B} \rightarrow \mathbf{E}', \mathbf{B}'$, etc.

\mathbf{E}'_1 is the RCPL traveling in the $-z$ direction, and \mathbf{E}'_2 is the LCPL traveling in the $+z$ direction. The boundary conditions to match, for normal incidence of the *real* EM fields, are

$$\text{At } (z = 0): \quad \mathbf{E}'_1 = -\mathbf{E}'_2, \quad \mathbf{B}'_1 = \mathbf{B}'_2. \quad (\text{H15})$$

The complex EM waves for this (–) standing wave can then be written as

$$\tilde{\mathbf{E}}'_1 = E'_1(-\hat{\mathbf{x}} - i\hat{\mathbf{y}})e^{i(-k'_1z - \omega t)} \quad (\text{RCPL}), \quad (\text{H16a})$$

$$\tilde{\mathbf{E}}'_2 = E'_2(+\hat{\mathbf{x}} + i\hat{\mathbf{y}})e^{i(+k'_2z - \omega t)} \quad (\text{LCPL}), \quad (\text{H16b})$$

$$\tilde{\mathbf{B}}'_1 = +i\frac{n'_1}{c}\tilde{\mathbf{E}}'_1, \quad (\text{H16c})$$

$$\tilde{\mathbf{B}}'_2 = -i\frac{n'_2}{c}\tilde{\mathbf{E}}'_2, \quad (\text{H16d})$$

where ($E'_1, E'_2 \in \mathbb{R}$) are the amplitudes of the electric fields. Also,

$$\begin{aligned} k'_1 = k^R &= \frac{n^R\omega}{c}, \quad k'_2 = k^L = \frac{n^L\omega}{c}, \\ n'_1 = n^R, \quad n'_2 &= n^L. \end{aligned} \quad (\text{H17})$$

a. Calculating C_g^-

The optical chirality C_g^- is [see Eq. (19)]:

$$C_g^- = \left[\frac{\epsilon^-}{2} \mathbf{E}^- \cdot (\nabla \times \mathbf{E})^- + \frac{1}{2\mu^-} \mathbf{B}^- \cdot (\nabla \times \mathbf{B})^- \right]. \quad (\text{H18})$$

For simplicity, due to the presence of both left- and right-handed indices of refraction, we again utilize Eq. (H8):

$$\begin{aligned} \text{Im}(\tilde{\mathbf{E}}^* \cdot \tilde{\mathbf{B}})^- &= \text{Im}[(\tilde{\mathbf{E}}'_1 + \tilde{\mathbf{E}}'_2)^* \cdot (\tilde{\mathbf{B}}'_1 + \tilde{\mathbf{B}}'_2)] \\ &= \frac{1}{c} \text{Im}[in'_1|\tilde{\mathbf{E}}'_1|^2 - in'_2|\tilde{\mathbf{E}}'_2|^2 + in'_1\tilde{\mathbf{E}}'_1 \cdot (\tilde{\mathbf{E}}'_2)^* \\ &\quad - in'_2(\tilde{\mathbf{E}}'_1)^* \cdot \tilde{\mathbf{E}}'_2]. \\ \therefore \frac{2}{\epsilon^-}C_g^- &= -\frac{2\omega}{c}[n^R E_1'^2 - n^L E_2'^2 \\ &\quad + E'_1E'_2(n^L - n^R) \cos(zk_{\text{tot}})]. \end{aligned} \quad (\text{H19})$$

b. Calculating U_γ^-

Now let us calculate $\frac{2}{\epsilon^-}U_\gamma^-$ for the (–) configuration. Again, using Eqs. (H3):

$$|\tilde{\mathbf{E}}^-|^2 = (\tilde{\mathbf{E}}'_1 + \tilde{\mathbf{E}}'_2)^* \cdot (\tilde{\mathbf{E}}'_1 + \tilde{\mathbf{E}}'_2) = 2[(E'_1)^2 + (E'_2)^2 - 2E'_1E'_2 \cos(k_{\text{tot}}z)], \quad (\text{H20a})$$

$$\begin{aligned} |\tilde{\mathbf{B}}^-|^2 &= |\tilde{\mathbf{B}}'_1|^2 + |\tilde{\mathbf{B}}'_2|^2 + 2\text{Re}(\tilde{\mathbf{B}}'_1 \cdot \tilde{\mathbf{B}}'_2^*) \\ &= \frac{2}{c^2} [(n'_1E'_1)^2 + (n'_2E'_2)^2 + 2n'_1n'_2E'_1E'_2 \cos(k_{\text{tot}}z)]. \end{aligned} \quad (\text{H20b})$$

Then, from Eq. (23),

$$\begin{aligned} \frac{2}{\epsilon^-}U_\gamma^- &= \frac{1}{2} \left(|\tilde{\mathbf{E}}^-|^2 + \frac{\chi''}{\alpha''} |\tilde{\mathbf{B}}^-|^2 \right) \\ &= (E'_1)^2(1 + \gamma^R) + (E'_2)^2(1 + \gamma^L) \\ &\quad + 2E'_1E'_2(\sqrt{\gamma^L\gamma^R} - 1) \cos(k_{\text{tot}}z). \end{aligned} \quad (\text{H21})$$

APPENDIX I: KRAMERS-KRONIG TRANSFORMATION OF CD TO ORD

We begin with the Kramers-Kronig relations for optical rotation and CD that are given in Eqs. (5.2.35a) and (5.2.35b)

of Ref. [1]:

$$\text{ORD: } \Delta\theta(f_\omega) = +\frac{2\omega^2}{\pi} \text{P} \int_0^\infty \frac{\Delta\eta(g_\xi)}{\xi(\xi^2 - \omega^2)} d\xi, \quad (\text{I1a})$$

$$\text{CD: } \Delta\eta(g_\omega) = -\frac{2\omega^3}{\pi} \text{P} \int_0^\infty \frac{\Delta\theta(f_\xi)}{\xi^2(\xi^2 - \omega^2)} d\xi, \quad (\text{I1b})$$

where ω is the angular frequency of the incident light, P is the Cauchy principal value, and f and g are the dispersion and absorption line-shape functions, respectively, as described in Appendix C.

The integrals in Eqs. (I1) have a singularity at resonance, that is, $\xi \rightarrow \omega$, from the denominator term

$$(\xi^2 - \omega^2) = (\xi - \omega)(\xi + \omega).$$

However, it is a simple pole and cancels from both sides ($\xi \rightarrow \omega^-$ and $\xi \rightarrow \omega^+$) since the integrand is odd about ω , provided it is continuous. By removing this single point when $\xi = \omega$, which is the meaning of taking the ‘‘principal value’’ P, we obtain finite integrals.

We applied a Kramers-Kronig transformation of the CD data provided in the supporting online material for Ref. [2]. To do so, we fit the CD graph given, and numerically integrated our approximated fit to it, using Eqs. (I1) converted to integration over wavelength. We then converted $\Delta\theta$ to

$$\frac{\Delta n}{n_{\text{ave}}^0} = \frac{n^L - n^R}{n^L + n^R} = \frac{1}{2} \frac{n^L - n^R}{n_{\text{ave}}^0}, \quad (\text{I2})$$

with the help of Eqs. (5.2.3a) and (5.2.3b) from Ref. [1]:

$$\text{ORD: } \Delta\theta = \frac{\omega l}{2c} (n^L - n^R), \quad (\text{I3a})$$

$$\text{CD: } \eta = \frac{\omega l}{2c} (n'^L - n'^R), \quad (\text{I3b})$$

where l is the path length of the material traversed.

We assumed that the CD data given was complete spectrally, that is, CD was zero outside of the range given (430–580 nm). Though the full spectrum is required for Kramers-Kronig transformations to be accurate, this still provided very reasonable results. We also assumed the path length l to be 10 nm, as suggested in Ref. [2]. The CD spectrum and Kramers-Kronig transformed ORD spectrum for both m-enantiomer and p-enantiomer are shown in Fig. 10.

To be complete, we point out that the CD spectrum data (in the Supplemental Materials in Ref. [2]), is for a given concentration of chiral molecules. However, the dissymmetry factor measurements for the experiment would likely have a different concentration. In our case, we are concerned with obtaining the ratios, such as $g = (A^+ - A^-)/A_{\text{ave}}$ or $\Delta n/n_{\text{ave}}$. For these ratios then, the concentration would be canceled to a good approximation.

In particular, we are concerned with the ratio $\Delta n/n_{\text{ave}}^0$. In this case, $\Delta n/n_{\text{ave}}^0$ obtained from the CD and ORD spectrum data (from the supplemental materials) can be compared on equal footing with that obtained from the dissymmetry factor measurements in the main paper of Ref. [2]. The results of

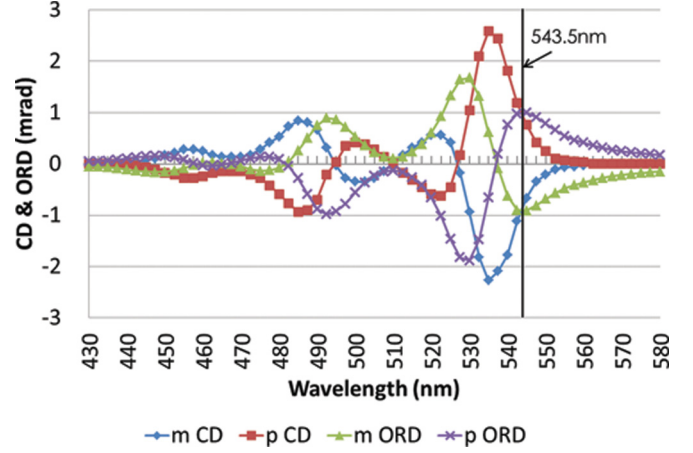


FIG. 10. (Color online) CD and Kramers-Kronig transformed ORD spectrum (in milliradians) for the m-enantiomer and p-enantiomer used in Ref. [2]. CD data are as given in the supporting online material for Ref. [2]. ORD spectrum was calculated via Kramers-Kronig transformation of the CD data.

our Kramers-Kronig transformed ORD calculations are now given. It is for the 543.5-nm wavelength laser field used in the experiment:

$$(n^L - n^R)_m \sim -0.0157, \quad (\text{I4a})$$

$$(n^L - n^R)_p \sim +0.0170, \quad (\text{I4b})$$

where m subscript is for the m-enantiomer, and p subscript is for the p-enantiomer in Ref. [2].

We would like to write this as a ratio over n_{ave} . To do so, since we do not know the value of the index of refraction for the enantiomers, we approximate as follows and use Eq. (I2):

$$(n_{\text{ave}}^0)_{\text{KKT}} = \left(\frac{n^L + n^R}{2} \right)_{\text{KKT}} \approx 1, \quad (\text{I5a})$$

$$\left(\frac{\Delta n}{n_{\text{ave}}^0} \right)_{\text{KKT}} \approx \frac{1}{2} (n^L - n^R), \quad (\text{I5b})$$

where ‘‘KKT’’ is for the Kramers-Kronig transformed fit from the CD data.

We then have

$$\left(\frac{\Delta n}{n_{\text{ave}}^0} \right)_{m,\text{KKT}} \approx -7.85 \times 10^{-3}, \quad (\text{I6a})$$

$$\left(\frac{\Delta n}{n_{\text{ave}}^0} \right)_{p,\text{KKT}} \approx +8.50 \times 10^{-3}, \quad (\text{I6b})$$

$$|\Delta_0| \equiv \left| \left(\frac{\Delta n}{n_{\text{ave}}^0} \right)_{\text{KKT}} \right|_{\text{ave}} \approx +8.18 \times 10^{-3}. \quad (\text{I6c})$$

These values are consistent with what we would expect from the order-of-magnitude estimation of Eq. (G5c).

- [1] L. Barron, *Molecular Light Scattering and Optical Activity*, 2nd ed. (Cambridge University Press, Cambridge, UK, 2004).
- [2] Y. Tang and A. E. Cohen, *Science* **332**, 333 (2011).
- [3] Y. Tang and A. E. Cohen, *Phys. Rev. Lett.* **104**, 163901 (2010).
- [4] D. M. Lipkin, *J. Math. Phys.* **5**, 696 (1964).
- [5] T. W. B. Kibble, *J. Math. Phys.* **6**, 1022 (1965).
- [6] D. Candlin, *Il Nuovo Cimento* **37**, 1390 (1965).
- [7] D. M. Fradkin, *J. Math. Phys.* **6**, 879 (1965).
- [8] K. Y. Bliokh and F. Nori, *Phys. Rev. A* **83**, 021803 (2011).
- [9] M. M. Coles and D. L. Andrews, *Phys. Rev. A* **85**, 063810 (2012).
- [10] R. P. Cameron, S. M. Barnett, and A. M. Yao, *New J. Phys.* **14**, 053050 (2012).
- [11] S. M. Barnett, R. P. Cameron, and A. M. Yao, *Phys. Rev. A* **86**, 013845 (2012).
- [12] N. Yang and A. E. Cohen, *J. Phys. Chem. B* **115**, 5304 (2011).
- [13] N. Yang, Y. Tang, and A. E. Cohen, *Nano Today* **4**, 269 (2009).
- [14] E. Hendry, R. V. Mikhaylovskiy, L. D. Barron, M. Kadodwala, and T. J. Davis, *Nano Lett.* **12**, 3640 (2012).
- [15] A. G. Smart, *Phys. Today* **64**, 16 (2011).
- [16] P. K. Jain, D. Ghosh, R. Baer, E. Rabani, and A. P. Alivisatos, *Proc. Natl. Acad. Sci. USA* **109**, 8016 (2012).
- [17] L. Novotny and B. Hecht, *Principles of Nano-optics* (Cambridge University Press, Cambridge, UK, 2006).
- [18] E. Hendry, T. Carpy, J. Johnston, M. Popland, R. V. Mikhaylovskiy, A. J. Laphorn, S. M. Kelly, L. D. Barron, N. Gadegaard, and M. Kadodwala, *Nat. Nanotechnol.* **5**, 783 (2010).
- [19] D. P. Craig and T. Thirunamachandran, *Molecular Quantum Electrodynamics: An Introduction to Radiation Molecule Interactions* (Dover, New York, 1998).
- [20] A. Salam, *Molecular Quantum Electrodynamics: Long-range Intermolecular Interactions* (Wiley & Sons, New York, 2010).
- [21] D. J. Griffiths, *Introduction to Electrodynamics*, 3rd ed. (Prentice Hall, New Jersey, 1999).
- [22] M. Born and E. Wolf, *Principles of Optics*, 6th ed. (Pergamon, Oxford, 1989).
- [23] J. W. Lewis, R. F. Tilton, C. M. Einterz, S. J. Milder, I. D. Kuntz, and D. S. Kliger, *J. Phys. Chem.* **89**, 289 (1985).
- [24] R. A. Goldbeck, D. B. Kim-Shapiro, and D. S. Kliger, *Annu. Rev. Phys. Chem.* **48**, 453 (1997).
- [25] J. Helbing and M. Bonmarin, *J. Chem. Phys.* **131**, 174507 (2009).
- [26] I. Eom, S.-H. Ahn, H. Rhee, and M. Cho, *Opt. Express* **19**, 10017 (2011).
- [27] H. Rhee, I. Eom, S.-H. Ahn, and M. Cho, *Chem. Soc. Rev.* **41**, 4457 (2012).
- [28] H. Rhee, Y.-G. June, J.-S. Lee, K.-K. Lee, J.-H. Ha, Z. H. Kim, S.-J. Jeon, and M. Cho, *Nature (London)* **458**, 310 (2009).
- [29] I. Eom, S.-H. Ahn, H. Rhee, and M. Cho, *Phys. Rev. Lett.* **108**, 103901 (2012).
- [30] H. Rhee, J.-H. Ha, S.-J. Jeon, and M. Cho, *J. Chem. Phys.* **129**, 094507 (2008).
- [31] H. Rhee, Y.-G. June, Z. H. Kim, S.-J. Jeon, and M. Cho, *J. Opt. Soc. Am. B* **26**, 1008 (2009).
- [32] H. Rhee, S.-S. Kim, S.-J. Jeon, and M. Cho, *ChemPhysChem* **10**, 2209 (2009).
- [33] H. Rhee, J.-H. Choi, and M. Cho, *Acc. Chem. Res.* **43**, 1527 (2010).
- [34] P. H. Vaccaro, *Nature (London)* **458**, 289 (2009).